Chapter 3
Stability Analysis

Abstract The focus of this chapter is the stability analysis of axially moving materials. There are many similarities with classical stability analysis of structures, like the buckling of beams and plates. However, the axial motion introduces the effects of inertia, bringing out many challenges that are discussed in this chapter. The chapter is divided as follows. In the first section, we will look into the history of stability investigations, concentrating on moving materials and especially on the extensive studies performed in this field during the last century. In the second section, we will introduce linear stability analysis using Bolotin's concept of dynamical stability. Finally, in the last three sections, dynamic and static stability analyses will be applied to moving membranes and plates.

3.1 Historical View of Stability Investigations

Stability analysis comes with a long tradition. The steady-state stability of parabolic shapes partially immersed in a homogeneous medium was analyzed in the two-part book *On Floating Bodies* by Archimedes of Syracuse. The book, originally dating from the third century BCE, can be thought of as the oldest surviving work on stability analysis; its probable application was shipbuilding (Russo 2004).

The present form of static stability analysis, which will be applied in this book, was originally developed by Euler (1766), for a differential equation describing the bending of a beam. The dynamic stability analysis for linear elastic systems, which extends Euler's method, is due to Bolotin (1963). According to Mote and Wickert (1991), the instability behaviour of some axially moving materials is mathematically analogous to the buckling of a compressed column, enabling the use of these techniques.

In the following, we will limit the scope of our consideration to moving materials. The first investigation in this area was performed by Skutch (1897) being published originally in German. The first English-language paper on the topic was published

N. Banichuk et al., *Mechanics of Moving Materials*,
Solid Mechanics and Its Applications 207, DOI: 10.1007/978-3-319-01745-7_3,

half a century later by Sack (1954). Both of these studies discussed the vibrations of a travelling string. Interest in the field then arose quickly. In a short study a few years later, by Archibald and Emslie (1958), two ways to derive the travelling string equation were presented. The first analytical solution to the travelling string problem concerned the free vibrations. It was obtained by Swope and Ames (1963), using a coordinate transform approach.

The dynamic and stability considerations discussed here were first reviewed in the article by Mote (1972). Natural frequencies are commonly analyzed together with the stability. The effects of axial motion of the web on its frequency spectrum and eigenfunctions were investigated in the papers by Archibald and Emslie (1958) and by Simpson (1973). It was shown that the natural frequency of each mode decreases when the transport speed increases, and that the travelling string and beam both experience divergence instability at a sufficiently high speed. However, in the case of the string, this result was recently contrasted by Wang et al. (2005), who showed using Hamiltonian mechanics that the ideal string remains stable at any speed. Travelling beams have been further analyzed by Parker (1998) in his study on gyroscopic continua, and by Kong and Parker (2004), where an approximate analytical expression was derived for the eigenfrequencies of a moving beam with small flexural stiffness.

Response predictions have been made for particular cases where the excitation assumes special forms, such as harmonic support motion (Miranker 1960) or a constant transverse point force (Chonan 1986). Arbitrary excitations and initial conditions were analyzed with the help of modal analysis and a Green's function method in the article by Wickert and Mote (1990). As a result, the critical speeds for travelling strings and beams were explicitly determined.

The loss of stability was studied with an application of dynamic and static approaches in the article by Wickert (1992). It was shown by means of numerical analysis that in all cases instability occurs when the frequency is zero and the critical velocity coincides with the corresponding velocity obtained from static analysis.

Two-dimensional studies have also been performed from the 1990s onwards. For example, Lin and Mote (1995) studied an axially moving membrane in a 2D formulation, predicting the equilibrium displacement and stress distributions under transverse loading. In the article by Shin et al. (2005), out-of-plane vibrations of an axially moving membrane were studied. They also found by numerical analysis that for a membrane with no-friction boundary conditions in the lateral direction along the rollers, the membrane remains dynamically stable until the critical speed, at which static instability occurs, is reached. Lin and Mote (1996) extended their study, predicting a wrinkling instability and the corresponding wrinkled shape of a web with small flexural stiffness. Lin (1997) continued the studies of stability.

It was realized early on that the vibration problem for an axially moving continuum is not the conventional one. Because of the longitudinal continuity of the material, the equation of motion for transverse vibration will contain additional terms, representing a Coriolis force and a centripetal force acting on the material. As a consequence, the resonant frequencies will be dependent on the longitudinal velocity of the axially

moving continuum, as was noted by Archibald and Emslie (1958), as well as Swope and Ames (1963), Simpson (1973), and Mujumdar and Douglas (1976).

In the 1980s, it was discovered that another important factor affecting the stability of the axially moving continuum, especially if the material itself is lightweight, is the interaction between the moving continuum and the surrounding medium (Pramila 1986). The interaction between the travelling continuum and the surrounding air is known to influence the critical velocity (Pramila 1986; Frondelius et al. 2006) and the dynamical response (Kulachenko et al. 2007b), possibly also affecting the divergence (buckling) shape. The mentioned studies concentrate on paper making, but the same phenomenon is encountered also in other applications. For example, in a paper by Hosaka and Crandall (1992), the vibrations of an elastic disc rotating above an air film were investigated.

The simplest approach to taking into account the fluid–structure interaction is to assume potential flow; that is, the surrounding air is assumed to be incompressible and inviscid, and the flow is assumed to be irrotational (like in e.g. Niemi and Pramila 1986). Experimental studies and some theoretical estimations (see, e.g., Pramila 1986) indicate that in the case of normal vibration, comparison of experimental and theoretical results shows that predictions based on the potential flow theory are within about 10 % of the measured results. To solve the external hydrodynamic problem, and to find the reaction of the surrounding medium, the finite element method has been used (e.g. Niemi and Pramila 1986).

A closely related problem is the response of stationary material to a surrounding axial flow. It has been noted Païdoussis (2008) that this problem, in turn, is related to the canonical problem of the fluid-conveying pipe. However, the case of material surrounded by axial flow is more complicated than the case of the pipe, due to the nonlocal nature of the aerodynamic reaction. The problems of slender structures in axial flow have been studied extensively, and are summarized in the two-volume book by Païdoussis (1998, 2004).

Returning to moving materials, the dynamical properties of moving plates have been studied by Shen et al. (1995) and by Shin et al. (2005), and the properties of a moving paper web have been studied in the two-part article by Kulachenko et al. (2007a,b). Critical regimes and other problems of stability analysis have been studied by Wang (2003) and Sygulski (2007).

Results that axially moving beams experience divergence instability at a sufficiently high beam velocity have been obtained also for beams interacting with external media; see, e.g., Chang and Moretti (1991), and Banichuk et al. (2010b, 2011b); Jeronen (2011). The same authors have extended the study in Banichuk et al. (2010a, 2011a), for a two-dimensional model of the web, considered as a moving plate under homogeneous tension but without external media. These studies have been further extended in Banichuk et al. (2013) and Tuovinen (2011) to the case with a linear non-homogeneous tension distribution (see also Chap. 4).

The mechanical behavior of a paper web under a non-failure condition is adequately described by the model of an elastic orthotropic plate. The rigidity coefficients of the plate model that describe the tension and bending of the paper sheet have been estimated for various types of paper in many publications. See, for

example, the articles by Göttsching and Baumgarten (1976), by Thorpe (1981), by Skowronski and Robertson (1985) and by Seo (1999). The deformation properties of a sheet of paper under tensile stress or strain are used in simulation of axial movement of a paper web. In particular, these properties are important for the modeling of the instability of the web.

In a recent article by Hatami et al. (2009), the free vibration of a moving orthotropic rectangular plate was studied at sub- and supercritical speeds, and its flutter and divergence instabilities at supercritical speeds. The study is limited to simply supported boundary conditions at all edges. For the solution of equations of orthotropic moving material, many necessary fundamentals can be found in the book by Marynowski (2008).

The free vibrations of stationary orthotropic rectangular plates have been extensively studied. The classical reference work in this area is the book by Gorman (1982). More recently, Biancolini et al. (2005) included in their study all combinations of simply supported and clamped boundary conditions on the edges. Xing and Liu (2009) obtained exact solutions for the free vibrations of stationary rectangular orthotropic plates. They considered three combinations of simply supported (S) and clamped (C) boundary conditions: SSCC, SCCC, and CCCC. Kshirsagar and Bhaskar (2008) studied vibrations and buckling of loaded stationary orthotropic plates. They found critical loads of buckling for all combinations of boundary conditions S, C, and F.

Recently, attention has turned toward the material model, which is also an important factor in the stability behaviour of a moving material. Industrial materials often have viscoelastic characteristics (see, e.g., Fung et al. 1997), and consequently, viscoelastic moving materials have been recently studied widely. In paper making, wet paper webs are highly viscous, and therefore, viscoelasticity should be taken into account in the models (see, e.g., Alava and Niskanen 2006). Also plasticity is known to occur (see, e.g., Erkkilä et al. 2013); however that topic is beyond the scope of the present book.

First studies on transverse vibration of viscoelastic material traveling between two fixed supports were done by Fung et al. (1997), using a string model. Extending the work, they studied the material damping effect in Fung et al. (1998).

Several studies on travelling viscoelastic materials, concerning strings and beams, have been performed during the last decade. Chen and Zhao (2005) represented a modified finite difference method to simplify a non-linear model of an axially moving viscoelastic string. They studied the free transverse vibrations of elastic and viscoelastic strings numerically.

Oh et al. (2004) and Lee and Oh (2005) studied critical speeds, eigenvalues, and natural modes of axially moving viscoelastic beams using the spectral element model. They analyzed dynamic behavior of axially moving viscoelastic beams using modal analysis, performed a detailed eigenfrequency analysis, and reported that viscoelasticity did not affect the critical velocity of the beam.

Marynowski and Kapitaniak (2002) compared two different internal damping models in modeling of moving viscoelastic (non-linear) beams. For the linearized Kelvin–Voigt model, it was found that the beam exhibits divergent instability at some critical speed. In the case of non-linear BÃŒrgers model, the critical speed decreased

when the internal damping was increased, and the beam was found to experience the first instability in the form of flutter.

A few studies on transverse vibrations of axially moving viscoelastic plates have also been done. Very recently, Yang et al. (2012) studied vibrations, bifurcation and chaos of axially moving viscoelastic plates using finite differences and a non-linear model for transverse displacements. They concentrated on bifurcations and chaos, but also studied the dynamic characteristics of a linearised elastic model with the help of eigenfrequency analysis.

A particular question about whether one should use the material time derivative or the partial time derivative in the viscoelastic constitutive relations for moving materials, has recently been discussed especially in the case of the widely used Kelvin–Voigt material model. Mockensturm and Guo (2005) suggested that the material derivative should be used. They studied non-linear vibrations and dynamic response of axially moving viscoelastic strings, and found significant discrepancy in the frequencies at which non-trivial limit cycles exist, comparing the models with the partial time derivative to those with the material time derivative.

Recently, the material derivative has been used in most of the studies concerning axially moving viscoelastic beams (see e.g. the papers by Chen et al. 2008, Chen and Ding 2010, Chen and Wang 2009, and Ding and Chen 2008). Kurki and Lehtinen (2009) suggested, independently, that the material derivative in the constitutive relations should be used in their study concerning the in-plane displacement field of a traveling viscoelastic plate. Some more studies specifically about viscoelastic moving materials will be introduced in Chap. 5.

3.2 Linear Stability Analysis

The most straightforward and efficient way to study stability is to use linear stability analysis. It is well-known that the normal vibrations of an elastic linear system are time-harmonic (this is noted by e.g., Xing and Liu 2009). For the stability analysis of all such systems described by partial differential equation models, it is standard to use the time-harmonic trial function

$$w(x,t) = \exp(st)\, W(x)\ , \tag{3.1}$$

where s is complex, $W(x)$ is an unknown eigenmode to be determined and x is a scalar or a vector depending on the dimensionality of the problem. This removes the time dependence from the partial differential equation, making it sufficient to solve a (pseudo-)steady-state problem including the unknown scalar s, the allowed values of which are determined implicitly by the boundary conditions and problem parameters. The resulting equation will be a partial differential equation in space, but polynomial with respect to s.

The trial function (3.1) produces a complex-valued solution $w(x,t)$. The space component $W(x)$ is typically real-valued for stationary materials, and complex-valued

for moving materials. It is easy to see that in the case of linear partial differential equations with real-valued coefficients, the real and imaginary components of $w(x,t)$ will also be solutions of the original problem. Let $\mathcal{L}$ be a linear differential operator. For example, for the real part, we have

$$\begin{aligned} \mathrm{Re}\,(\mathcal{L}(w)) &= \mathrm{Re}\,[\mathcal{L}(\,\mathrm{Re}\,(w) + i\,\mathrm{Im}\,(w)\,)] \\ &= \mathrm{Re}\,[\mathcal{L}(\mathrm{Re}\,(w)) + i\,\mathcal{L}(\mathrm{Im}\,(w))] \\ &= \mathcal{L}(\mathrm{Re}\,(w))\,, \end{aligned} \tag{3.2}$$

where the last equality holds only if the coefficients of $\mathcal{L}$ are real. The same observation holds for the imaginary part. Thus, both Re $w(x,t)$ and Im $w(x,t)$ are real-valued solutions of the original problem.

However, for moving materials, the real and imaginary components of $W(x)$ are typically not solutions of the auxiliary steady-state problem: using the trial function (3.1), only the full complex-valued solution $W(x)$ is valid for the auxiliary problem. It is only the complete solution $w(x,t)$ whose real and imaginary components satisfy the original problem separately. For an example of this, the properties stated here can be easily verified for the analytical free vibration solution given in Sect. 2.1.1 for the constant-coefficient travelling string. The reason is, of course, that the stability exponent s is complex.

The allowed values of the *stability exponent* s completely characterize the free vibrations of the elastic linear system under consideration. Consider the problem parameters fixed. If Re $s \leq 0$ for all solutions (s, W), the system is *stable* and undergoes time-harmonic vibration. If Re $s < 0$ for one or more solutions (s, W), these solutions also contain a damping component. If Re $s > 0$ for at least one solution (s, W), the system is *unstable* (Bolotin 1963).

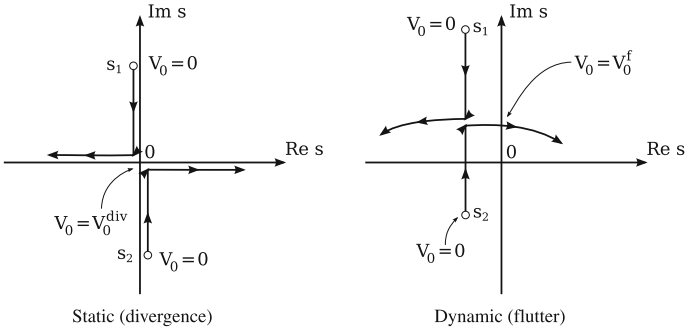

Fig. 3.1 Behaviour of the stability exponent s for the two different instability types in the classification due to Bolotin (1963). The *arrows* show the motion of the eigenvalues s_j as the problem parameter V_0 is increased quasistatically. In the *left picture*, the symbols are drawn off the axes for legibility reasons only; $s^2 \in \mathbb{R}$ for all V_0. In the *right picture*, the real part is initially negative. In both cases, the eigenvalues merge at the collision point, and then immediately separate

Based on the trial function (3.1) we can make the distinction of *static* versus *dynamic* instability, depending on whether Im $s = 0$ in the critical state. This classification is due to Bolotin (1963). The concepts are illustrated in Fig. 3.1.

Roughly speaking, the *critical state* can be defined as follows. We begin in some initially stable state of the system. For axially travelling materials, the initial state is usually taken as axial velocity $V_0 = 0$. We then start increasing the problem parameter of interest, call it p, quasistatically. After a while, the parameter p has reached a value p_0. If there exists at least one solution (s, W) such that Re $s > 0$ for all $p = p_0 + \varepsilon$ with arbitrarily small $\varepsilon > 0$, but Re $s \leq 0$ for all solutions s for $p = p_0 - \varepsilon$, the value p_0 is called the *critical* parameter value. It is the point of transition from stable to unstable behaviour.

Assume we have found a critical parameter value $p = p_0$. If Im $s = 0$ just above the critical value, $p = p_0 + \varepsilon$, the complex-valued exp in (3.1) simplifies to a real-valued exp, and the displacement will grow exponentially with time. This is called *static instability* or *divergence* (Fig. 3.1, left). This corresponds to s passing through the origin of the complex plane, and thus the critical states for this kind of instability can be found by a steady-state analysis (see Bolotin 1963, or consider (3.1) for $s = 0$).

Often the existence of a nontrivial steady-state solution is taken as indication of an instability, and e.g. the buckling analysis of travelling panels and plates is based on this idea. However, in their analysis of the travelling ideal string, Wang et al. (2005) caution that steady-state solutions may exist without indicating an instability, if the eigenfunctions remain linearly independent at the critical parameter value. Thus, we may conclude that a static instability can only arise from a steady state, but in a rigorous analysis, the existence of a steady state should be taken only as a necessary condition for static instability, not a sufficient one.

If Im $s \neq 0$ for $p = p_0 + \varepsilon$, the complex-valued exp in (3.1) becomes a product of a real-valued exp and a harmonic component, e.g. sin, cos or a linear combination of these. In this case, the displacement will exhibit exponentially growing vibrations with time (see Fig. 3.1, right). This is called *dynamic instability* or *flutter*. This should not be confused with the engineering use of the term *flutter* to describe also stable vibrations.

Linear perturbation analysis around the critical parameter value is one method that can be used to confirm that the critical state indeed indicates an instability for $p = p_0 + \varepsilon$ (see e.g. the analysis of Parker 1998, for the moving beam). Another method is to compute the complex eigenfrequencies of the system, based on the trial function (3.1), for a range of parameter values $[p_0 - \varepsilon,\ p_0 + \varepsilon]$.

In the case of stability analysis of linear partial differential equations, it is evident from the linear superposition property that solution components which obviously always stay bounded may be discarded without further consideration. Thus, linear stability analysis can be focused on the solution components for which the boundedness of the long-term behaviour, under various different values for the problem parameters, is nontrivial.

Finally, it should be noted that for the investigation of small vibrations of elastic systems, linearized models are often used. If system enters an unstable state, the

small displacement assumption eventually breaks, possibly very quickly. From that point on, the model no longer describes the physics of the situation being analyzed. It is generally agreed that linearized small-displacement models are sufficient up to the first instability (see e.g. Païdoussis 2005).

3.3 Dynamic Analysis of Moving Membranes and Plates

From experimental studies and some theoretical estimations, it is known that mechanical instability of a travelling paper web can arise at some critical velocities, and that the instability may occur in either dynamic, i.e. flutter, or static, i.e. divergence, forms. These critical velocities are of both theoretical and practical interest, as they set an upper limit for the running speed of paper machines, and consequently, for the rate of paper production that can be achieved. Some previous investigations show that for an axially moving elastic paper web under a homogeneous tension profile along the rollers and certain other conditions, the value of divergence speed V_0^{div} is smaller than the value of flutter speed V_0^{fl}, and hence the critical instability will be of the divergence type.

In this section, the focus is on how to analyze the dynamic problem of stability. We will follow the method described by Bolotin (1963). Recall the equation of small transverse vibrations of the travelling plate subjected to homogeneous tension, (2.12). We represent it as follows:

$$\frac{\partial^2 w}{\partial t^2} + 2V_0 \frac{\partial^2 w}{\partial x \partial t} + \left(V_0^2 - C^2\right) \frac{\partial^2 w}{\partial x^2} + \frac{D_0}{m} \mathcal{L}_0(w) = 0 \,, \qquad C = \sqrt{\frac{T_0}{m}} \,, \tag{3.3}$$

where $w = w(x, t)$ is the transverse displacement, and the orthotropic bending operator is

$$\mathcal{L}_0(w) = \frac{D_1}{D_0} \frac{\partial^4 w}{\partial x^4} + \frac{2D_3}{D_0} \frac{\partial^4 w}{\partial x^2 \partial y^2} + \frac{D_2}{D_0} \frac{\partial^4 w}{\partial y^4} \,. \tag{3.4}$$

Here D_j for $j = 1, 2, 3$ are the orthotropic bending rigidities

$$D_1 = \frac{h^3}{12} C_{11} \,, \quad D_2 = \frac{h^3}{12} C_{22} \,, \quad D_3 = \frac{h^3}{12} \left(C_{12} + 2\, C_{66}\right) \,,$$

which were already introduced as (2.18), Sect. 2.1.3 (or see Timoshenko and Woinowsky-Krieger 1959, Chap. 11). The C_{ij} are the elastic moduli, (2.19). The quantity D_0 is a normalization constant, for which we have chosen the value $D_0 = D_1$.

The boundary value problem consisting of (3.3)–(3.4) with the boundary conditions (2.20)–(2.22) is homogeneous and invariant with respect to the symmetry operation $y \to -y$ and, consequently, all solutions of the problem are either symmetric or antisymmetric functions of y, i.e.

$$w(x, y, t) = w(x, -y, t) \qquad \text{or} \qquad w(x, y, t) = -w(x, -y, t) \ . \tag{3.5}$$

In the following analysis, however, this symmetry property is not necessary.

Using the time-harmonic trial function (3.1), we can represent the solution of our dynamic boundary-value problem (3.3)–(3.4), (2.20)–(2.22) as

$$w(x, y, t) = W(x, y)e^{i\omega t} = W(x, y)e^{st} \ , \tag{3.6}$$

where ω is the angular frequency of small transverse vibrations and $s = i\omega$ is the stability exponent. As presented in the previous section, Sect. 3.2, if s is purely imaginary and consequently ω is real, the membrane or plate performs harmonic vibrations of a small amplitude and its motion can be considered stable. If, for some values of the problem parameters, the real part of the stability exponent becomes positive, the transverse vibrations grow exponentially and consequently the behaviour is unstable (See Fig. 3.1, left).

3.3.1 Dynamic Stability of Membranes

Classical approach for modelling of moving materials is to apply the model of a travelling membrane. In the case of a membrane, efficient analytical methods are usually available. We begin the analysis of the moving membrane by defining the corresponding eigenvalue problem. Homogeneous tension is applied at the boundaries $x = 0$ and $x = \ell$. In order to investigate the dynamic behavior, we insert the representation (3.6) into (3.3). Since the case of a membrane is considered, we omit the bending rigidity terms from (3.3), i.e., $(D_0/m)\,\mathcal{L}_0(w) = 0$. We obtain the following equation for small time-harmonic vibrations of the travelling membrane:

$$s^2 W + 2sV_0 \frac{\partial W}{\partial x} + \left(V_0^2 - C^2\right) \frac{\partial^2 W}{\partial x^2} = 0 \ , \tag{3.7}$$

with zero displacement boundary conditions

$$(W)_{x=0,\,\ell} = 0 \ , \quad -b \le y \le b \ . \tag{3.8}$$

We will see that the choice of boundary conditions in the y direction, on the edges $\{0 \le x \le \ell, \ y = \pm b\}$, does not matter in the following analysis.

We multiply (3.7) by W and perform integration over the domain

$$\Omega \equiv \left\{(x, y) \in \mathbb{R}^2 \ | \ 0 < x < \ell, \ -b < y < b\right\} \tag{3.9}$$

to obtain

$$s^2 \int_\Omega W^2 \, \mathrm{d}\Omega + 2sV_0 \int_\Omega W \frac{\partial W}{\partial x} \, \mathrm{d}\Omega + \left(V_0^2 - C^2\right) \int_\Omega W \frac{\partial^2 W}{\partial x^2} \, \mathrm{d}\Omega = 0 \, . \quad (3.10)$$

It is worth noting that the problem (3.10) is a special case of the variational form of the original eigenvalue problem (3.7). In (3.10), we only test against W itself, not against an arbitrary test function. However, any solution of the original problem (3.7) is also a solution of (3.10). Hence, the eigenvalues of problem (3.10) include the eigenvalues of problem (3.7), i.e. we may get additional solutions. As we are interested in the behavior of the eigenvalues of problem (3.7), it is sufficient to notice that if all the eigenvalues of problem (3.10) have similar behaviour with each other, then the eigenvalues of (3.7) have the same behaviour.

The second and third integrals in (3.10) are evaluated with integration by parts and the boundary conditions (3.8):

$$\begin{aligned} \int_\Omega W \frac{\partial W}{\partial x} \, \mathrm{d}\Omega &= \int_{-b}^{b} \int_0^{\ell} W \frac{\partial W}{\partial x} \, \mathrm{d}x \, \mathrm{d}y \\ &= \int_{-b}^{b} \left[\frac{W^2(\ell, y)}{2} - \frac{W^2(0, y)}{2} \right] \mathrm{d}y \\ &= 0 \, , \end{aligned} \quad (3.11)$$

and

$$\int_\Omega W \frac{\partial^2 W}{\partial x^2} \, \mathrm{d}\Omega = - \int_\Omega \left(\frac{\partial W}{\partial x} \right)^2 \mathrm{d}\Omega \, . \quad (3.12)$$

Using (3.10)–(3.12) and performing elementary transformations, we obtain the following expression for the stability exponent:

$$s^2 = \left(V_0^2 - C^2\right) \frac{\int_\Omega \left(\frac{\partial W}{\partial x} \right)^2 \mathrm{d}\Omega}{\int_\Omega W^2 \, \mathrm{d}\Omega} \, . \quad (3.13)$$

If s becomes zero, we have a steady state solution (divergence) with frequency $\omega = 0$ at the velocity $V_0 = V_0^{\mathrm{div}}$. From (3.13), the value of this divergence velocity is found as

$$V_0^{\mathrm{div}} = C = \sqrt{\frac{T_0}{m}} = \sqrt{\frac{hu_0}{m\ell} E_1} \, , \quad (3.14)$$

where in the last form, (2.40) from Sect. 2.2 has been used. Here u_0 is a prescribed displacement at $x = \ell$.

3.3.2 Dynamic Analysis of Small Transverse Vibrations and Elastic Stability of Isotropic Plates

To investigate the dynamic behaviour of the plate, we insert, following the membrane case, representation (3.6) into (3.3). As the object is a plate, the bending rigidities cannot be omitted. Therefore, for small time-harmonic vibrations of the travelling plate subjected to homogeneous tension, we have the equation

$$s^2 W + 2sV_0 \frac{\partial W}{\partial x} + (V_0^2 - C^2)\frac{\partial^2 W}{\partial x^2} + \frac{D}{m}\Delta^2 W = 0 \,. \tag{3.15}$$

Boundary conditions for the plate problem are

$$(W)_{x=0,\ell} = 0 \,, \qquad \left(\frac{\partial^2 W}{\partial x^2}\right)_{x=0,\ell} = 0 \,, \qquad -b \le y \le b \,, \tag{3.16}$$

$$\left(\frac{\partial^2 W}{\partial y^2} + \beta_1 \frac{\partial^2 W}{\partial x^2}\right)_{y=\pm b} = 0 \,, \qquad 0 \le x \le \ell \,, \tag{3.17}$$

$$\left(\frac{\partial^3 W}{\partial y^3} + \beta_2 \frac{\partial^3 W}{\partial x^2 \partial y}\right)_{y=\pm b} = 0 \,, \qquad 0 \le x \le \ell \,. \tag{3.18}$$

For an orthotropic plate, we have

$$\begin{aligned} \beta_1 &= \nu_{12} \,, \\ \beta_2 &= \nu_{12} + \frac{4\,G_{12}}{E_2}\,(1 - \nu_{12}\nu_{21}) \,. \end{aligned} \tag{3.19}$$

As was noted in Sect. 2.1.3, in the case of an isotropic plate, the parameters above become simplified as

$$\beta_1 = \nu \qquad \text{and} \qquad \beta_2 = 2 - \nu \,, \tag{3.20}$$

by setting $\nu_{12} = \nu_{21} = \nu$, $E_1 = E_2 = E$, $G_{12} = G$, and using the isotropic shear modulus relation $G = E/(2\,(1+\nu))$. Then, factoring $1 - \nu_{12}\nu_{21} = 1 - \nu^2 = (1+\nu)(1-\nu)$ and simplifying reduces (3.19) into (3.20).

Proceeding similarly as in the membrane case, we multiply (3.15) by W and perform integration over the domain Ω to obtain

$$\begin{aligned} s^2 \int_\Omega W^2 \,\mathrm{d}\Omega + 2sV_0 \int_\Omega W \frac{\partial W}{\partial x}\,\mathrm{d}\Omega + (V_0^2 - C^2)\int_\Omega W \frac{\partial^2 W}{\partial x^2}\,\mathrm{d}\Omega \\ + \frac{D}{m}\int_\Omega W \Delta^2 W \,\mathrm{d}\Omega = 0 \,. \end{aligned} \tag{3.21}$$

The same argument holds for the variational form as in the membrane case. Equation (3.21) can be seen as an eigenvalue problem for the pair (s, W) with the parameter V_0, producing a spectrum of complex eigenfrequencies s and eigenmodes W for the chosen value of V_0. Alternatively, (3.21) can be viewed as an eigenvalue problem for the pair (V_0, W) with the parameter s, when s is fixed to any such value that at least one complex eigenfrequency exists for at least one choice of V_0. For other choices of s, this second eigenvalue problem has no solution.

Previously, we have noted the Eqs. (3.11) and (3.12) for the membrane. By using Green's 2nd identity, the last integral in (3.21) can be transformed into

$$\int_\Omega W\Delta^2 W \, \mathrm{d}\Omega = \int_\Omega (\Delta W)^2 \, \mathrm{d}\Omega + \int_\Gamma \left(W \frac{\partial}{\partial n} \Delta W - \Delta W \frac{\partial W}{\partial n} \right) \mathrm{d}\Gamma \, , \tag{3.22}$$

where n is the exterior unit normal to the boundary Γ of the domain Ω. We divide the boundary Γ into four parts (see Fig. 3.2):

$$\begin{aligned} \Gamma_- &= \{0 \le x \le \ell, \ y = -b\}, \qquad \Gamma_r = \{x = \ell, \ -b \le y \le b\} \, , \\ \Gamma_+ &= \{0 \le x \le \ell, \ y = b\}, \qquad \Gamma_\ell = \{x = 0, \ -b \le y \le b\} \, . \end{aligned}$$

Admitting counterclockwise integration along Γ, we have

$$I = \int_\Gamma \left(W \frac{\partial}{\partial n} \Delta W - \Delta W \frac{\partial W}{\partial n} \right) \mathrm{d}\Gamma = I_- + I_r + I_+ + I_\ell \, . \tag{3.23}$$

Here

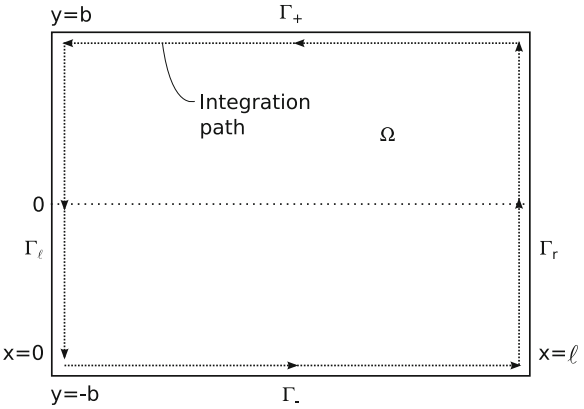

Fig. 3.2 Division of the boundary Γ for the investigated contour integral

$$I_r = I_\ell = 0 \,, \tag{3.24}$$

$$\begin{aligned} I_- &= \int_{\Gamma_-} \left(W \frac{\partial}{\partial n} \Delta W - \Delta W \frac{\partial W}{\partial n} \right) \mathrm{d}\Gamma \\ &= - \int_0^\ell \left(W \frac{\partial}{\partial y} \Delta W - \Delta W \frac{\partial W}{\partial y} \right)_{y=-b} \mathrm{d}x \,, \end{aligned} \tag{3.25}$$

$$\begin{aligned} I_+ &= \int_{\Gamma_+} \left(W \frac{\partial}{\partial n} \Delta W - \Delta W \frac{\partial W}{\partial n} \right) \mathrm{d}\Gamma \\ &= - \int_\ell^0 \left(W \frac{\partial}{\partial y} \Delta W - \Delta W \frac{\partial W}{\partial y} \right)_{y=b} \mathrm{d}x \\ &= \int_0^\ell \left(W \frac{\partial}{\partial y} \Delta W - \Delta W \frac{\partial W}{\partial y} \right)_{y=b} \mathrm{d}x \,. \end{aligned} \tag{3.26}$$

where we have used the relations

$$\mathrm{d}\Gamma = \mathrm{d}x, \quad \frac{\partial}{\partial n} = -\frac{\partial}{\partial y} \quad \text{for } (x, y) \in \Gamma_- \,, \tag{3.27}$$

$$\mathrm{d}\Gamma = -\mathrm{d}x, \quad \frac{\partial}{\partial n} = \frac{\partial}{\partial y} \quad \text{for } (x, y) \in \Gamma_+ \,, \tag{3.28}$$

and

$$W = \Delta W = 0 \quad \text{for } (x, y) \in \Gamma_\ell + \Gamma_r \,. \tag{3.29}$$

We obtain

$$I = I_- + I_+ = \int_0^\ell \left(Q(W, W)_{y=b} - Q(W, W)_{y=-b} \right) \mathrm{d}x \,, \tag{3.30}$$

where

$$Q(w, v) \equiv v \frac{\partial}{\partial y} \Delta w - \Delta w \frac{\partial v}{\partial y} \,. \tag{3.31}$$

with the arbitrary functions v and w. Using the boundary conditions for an isotropic plate, (3.17) and (3.18), we find that

$$Q(W, W) = \frac{W \dfrac{\partial^3 W}{\partial y^3}}{\left(\dfrac{2 - \nu}{1 - \nu} \right)} + \frac{\dfrac{\partial W}{\partial y} \dfrac{\partial^2 W}{\partial y^2}}{\left(\dfrac{\nu}{1 - \nu} \right)} \,, \qquad \text{at } y = \pm b \,. \tag{3.32}$$

We can see from (3.32) that the function Q is antisymmetric with respect to the transformation $y \to -y$ for symmetric and antisymmetric functions W, and consequently,

$$Q(W, W)_{y=b} = -Q(W, W)_{y=-b} \, . \tag{3.33}$$

We observe that

$$I = 2 \int_0^\ell Q(W, W)_{y=b} \, \mathrm{d}x \, . \tag{3.34}$$

From (3.22) and (3.34), we obtain

$$\int_\Omega W \Delta^2 W \, \mathrm{d}\Omega = \int_\Omega (\Delta W)^2 \, \mathrm{d}\Omega + 2 \int_0^\ell Q(W, W)_{y=b} \, \mathrm{d}x \, , \tag{3.35}$$

and, furthermore

$$\begin{aligned} \omega^2 &= -s^2 \\ &= \frac{(C^2 - V_0^2) \int_\Omega \left(\frac{\partial W}{\partial x} \right)^2 \mathrm{d}\Omega + \frac{D}{m} \left(\int_\Omega (\Delta W)^2 \, \mathrm{d}\Omega + 2 \int_0^\ell Q_{y=b} \, \mathrm{d}x \right)}{\int_\Omega W^2 \, \mathrm{d}\Omega} \, . \end{aligned} \tag{3.36}$$

We can now observe from representation (3.36) the following equation for the divergence mode (buckling mode):

$$\left(V_0^{\mathrm{div}} \right)^2 = C^2 + \frac{D}{m} \frac{\int_\Omega (\Delta W)^2 \mathrm{d}\Omega + 2 \int_0^\ell Q_{y=b} \, \mathrm{d}x}{\int_\Omega \left(\frac{\partial W}{\partial x} \right)^2 \mathrm{d}\Omega} \, . \tag{3.37}$$

In particular, it follows from (3.37) that when the bending rigidity D is negligible, the critical velocity is the same as for the axially travelling string (see, e.g., Chang and Moretti 1991). From the result further above, see (3.14), we see that the same value for the critical velocity also applies to ideal membranes. For a membrane, the divergence velocity does not depend on W. Thus, any combination of modes may occur at the critical velocity for the special case of an ideal membrane under homogeneous tension. These observations generalize the analogous results for a cylindrical deformation, i.e. a flat panel model of an ideal membrane (see Banichuk et al. 2010b).

3.4 Divergence Instability of Isotropic Plates

Next we will consider the buckling problem of an axially moving isotropic plate. In many practical cases, this is a reasonable simplification. For divergence instability of axially moving orthotropic plates, see Sect. 3.5.

3.4.1 Eigenvalue Problem

In this section, we will study the divergence (static instability) of a travelling isotropic plate subjected to homogeneous tension. The problem is formulated as an eigenvalue problem of the partial differential equation

$$\left(mV_0^2 - T_0\right)\frac{\partial^2 W}{\partial x^2} + D\left(\frac{\partial^4 W}{\partial x^4} + 2\frac{\partial^4 W}{\partial x^2 \partial y^2} + \frac{\partial^4 W}{\partial y^4}\right) = 0 \tag{3.38}$$

with the boundary conditions (3.16)–(3.18) and (3.20) (Sect. 3.3.2). We will study static (i.e. divergence) instability, and therefore time-dependent terms are excluded from (3.3). In order to determine the minimal eigenvalue

$$\lambda = \gamma^2 = \frac{\ell^2}{\pi^2 D}\left(mV_0^2 - T_0\right) \tag{3.39}$$

of the problem (3.16)–(3.18), (3.38), and the corresponding eigenfunction $W = W(x, y)$, we apply the following representation:

$$W = W(x, y) = f\left(\frac{y}{b}\right)\,\sin\left(\frac{\pi x}{\ell}\right)\,, \tag{3.40}$$

where $f\,(y/b)$ is an unknown function. It follows from (3.40) that the desired buckling mode (steady-state solution) W satisfies the boundary condition (3.16). The half-sine shape of the solution in the longitudinal direction is well-known (see, e.g., the article by Lin 1997). Using the dimensionless quantities

$$\eta = \frac{y}{b}\,, \qquad \mu = \frac{\ell}{\pi b}\,, \tag{3.41}$$

and the relations (3.17)–(3.18) (Sect. 3.3.2) and (3.38)–(3.41), we obtain the following eigenvalue problem for the unknown function $f(\eta)$:

$$\mu^4\frac{\mathrm{d}^4 f}{\mathrm{d}\eta^4} - 2\mu^2\frac{\mathrm{d}^2 f}{\mathrm{d}\eta^2} + (1-\lambda)f = 0\,, \qquad -1 < \eta < 1\,, \tag{3.42}$$

$$\mu^2\frac{\mathrm{d}^2 f}{\mathrm{d}\eta^2} - \nu f = 0\,, \qquad \eta = \pm 1\,, \tag{3.43}$$

$$\mu^2\frac{\mathrm{d}^3 f}{\mathrm{d}\eta^3} - (2-\nu)\frac{\mathrm{d}f}{\mathrm{d}\eta} = 0\,, \qquad \eta = \pm 1\,, \tag{3.44}$$

where (3.43)–(3.44) represent the free-of-traction boundary conditions.

3.4.2 Analytical Solution

In this section, we will present the solution process of the eigenvalue problem (3.42)–(3.44). We consider the problem as a spectral boundary value problem. The problem is invariant with respect to the symmetry operation $\eta \to -\eta$, and consequently, all its eigenfunctions can be classified as

$$f^{\mathrm{s}}(\eta) = f^{\mathrm{s}}(-\eta), \quad f^{\mathrm{a}}(\eta) = -f^{\mathrm{a}}(-\eta), \quad 0 \le \eta \le 1 \,. \tag{3.45}$$

Here f^{s} and f^{a} are symmetric and antisymmetric (skew-symmetric) with respect to the x axis ($\eta = 0$). When $\gamma \le 1$, a divergence mode symmetric with respect to the x axis can be presented in the form

$$W = f^{\mathrm{s}}(\eta) \, \sin\left(\frac{\pi x}{\ell}\right) \tag{3.46}$$

where

$$f^{\mathrm{s}}(\eta) = A^{\mathrm{s}} \cosh\left(\frac{\kappa_+ \eta}{\mu}\right) + B^{\mathrm{s}} \cosh\left(\frac{\kappa_- \eta}{\mu}\right) \tag{3.47}$$

and

$$\kappa_+ = \sqrt{1+\gamma} \,, \quad \kappa_- = \sqrt{1-\gamma} \,. \tag{3.48}$$

The function $f^{\mathrm{s}}(\eta)$ is a symmetric solution of (3.42), and A^{s} and B^{s} are arbitrary constants. At first, we concentrate on the symmetric case and return to the antisymmetric case later.

Using the relations (3.43)–(3.47), we can derive the linear algebraic equations for determining the constants A^{s} and B^{s}:

$$A^{\mathrm{s}}\left(\kappa_+^2 - \nu\right) \cosh\left(\frac{\kappa_+}{\mu}\right) + B^{\mathrm{s}}\left(\kappa_-^2 - \nu\right) \cosh\left(\frac{\kappa_-}{\mu}\right) = 0 \,, \tag{3.49}$$

$$-A^{\mathrm{s}}\kappa_+\left(\kappa_-^2 - \nu\right) \sinh\left(\frac{\kappa_+}{\mu}\right) - B^{\mathrm{s}}\kappa_-\left(\kappa_+^2 - \nu\right) \sinh\left(\frac{\kappa_-}{\mu}\right) = 0 \,. \tag{3.50}$$

The condition for a non-trivial solution to exist in the form (3.46)–(3.48) is that the determinant of the system (3.49)–(3.50) must vanish. This is seen by observing that (3.49)–(3.50) is a homogeneous system of linear equations in A^{s}, B^{s}:

$$\begin{bmatrix} K_{11} & K_{12} \\ K_{21} & K_{22} \end{bmatrix} \begin{bmatrix} A^{\mathrm{s}} \\ B^{\mathrm{s}} \end{bmatrix} = \begin{bmatrix} 0 \\ 0 \end{bmatrix} \,, \tag{3.51}$$

where the coefficients K_{ij} are given by the obvious identifications. From linear algebra, it is known that a non-trivial solution satisfying (3.51) can only exist if the matrix $\mathbf{K}$ is singular. Hence its determinant must be zero.

This zero determinant condition leads to the transcendental equation

$$\kappa_- \left(\kappa_+^2 - \nu\right)^2 \cosh\left(\frac{\kappa_+}{\mu}\right) \sinh\left(\frac{\kappa_-}{\mu}\right) - \kappa_+ \left(\kappa_-^2 - \nu\right)^2 \sinh\left(\frac{\kappa_+}{\mu}\right) \cosh\left(\frac{\kappa_-}{\mu}\right) = 0 \,, \tag{3.52}$$

which determines the eigenvalues

$$\lambda = \gamma^2 \tag{3.53}$$

implicitly. Equation (3.52) can be transformed into a more convenient form,

$$\Phi(\gamma, \mu) - \Psi(\gamma, \nu) = 0 \,, \tag{3.54}$$

where we have defined

$$\Phi(\gamma, \mu) = \tanh\left(\frac{\sqrt{1-\gamma}}{\mu}\right) \coth\left(\frac{\sqrt{1+\gamma}}{\mu}\right) \tag{3.55}$$

and

$$\Psi(\gamma, \nu) = \frac{\sqrt{1+\gamma}\,(\gamma + \nu - 1)^2}{\sqrt{1-\gamma}\,(\gamma - \nu + 1)^2} \,. \tag{3.56}$$

Let us consider the modes of buckling which are antisymmetric about the x axis:

$$W = f^{\mathrm{a}}(\eta) \sin\left(\frac{\pi x}{\ell}\right) \,, \tag{3.57}$$

where

$$f^{\mathrm{a}}(\eta) = A^{\mathrm{a}} \sinh\left(\frac{\kappa_+ \eta}{\mu}\right) + B^{\mathrm{a}} \sinh\left(\frac{\kappa_- \eta}{\mu}\right) \tag{3.58}$$

for $\gamma \leq 1$. The values κ_+ and κ_- are defined by the expressions (3.48). Using the expression (3.58) for f^{a} and the boundary conditions on the free edges of the plate (3.43)–(3.44), we obtain the following transcendental equation for determining the quantity γ:

$$\Phi(\gamma, \mu) - \frac{1}{\Psi(\gamma, \nu)} = 0 \,. \tag{3.59}$$

In (3.59), $\Phi(\gamma, \mu)$ and $\Psi(\gamma, \nu)$ are again defined by the formulas (3.55) and (3.56). In the segment $0 < \gamma \leq 1$ being considered, the equation has two roots,

$$\gamma = \gamma_1 \quad \rightarrow \quad \gamma_0 < \gamma_1 < 1 \tag{3.60}$$

and

$$\gamma = \gamma_2 \quad \rightarrow \quad \gamma_2 = 1 \,, \tag{3.61}$$

for arbitrary values of the Poisson ratio ν and the geometric parameter μ. By using (3.60)–(3.61) and some properties described in the next section, it is possible to determine that

$$\gamma_* < \gamma_1 < \gamma_2 \,, \tag{3.62}$$

where γ_* is the minimal eigenvalue for the symmetric case. Thus, the critical buckling mode is symmetric with respect to the x axis, and corresponds to $\gamma = \gamma_*$, i.e., to the solution of (3.54). Hence we will limit our consideration to the symmetric case.

We have obtained an equation determining the minimal eigenvalue γ_*, (3.54). By relation (3.39), the corresponding critical velocity of the travelling band is then represented as

$$(V_0^{\text{div}})^2 = \frac{T_0}{m} + \frac{\gamma_*^2}{m}\left(\frac{\pi^2 D}{\ell^2}\right) \,. \tag{3.63}$$

In order to obtain the corresponding eigenmode, either A^{s} or B^{s} can be solved from either of the equations (3.49)–(3.50), and the other one (either B^{s} or A^{s}, respectively) can be chosen arbitrarily; it is the free coefficient of the eigenvalue problem. Finally, inserting the obtained γ_*, A^{s} and B^{s} into (3.46–3.47) gives the eigenmode corresponding to the eigenvalue γ_*.

One of A^{s} or B^{s} is left free, because the zero determinant condition holds at the value of $\gamma = \gamma_*$ that is a solution of (3.54). Hence, at $\gamma = \gamma_*$, the equations (3.49)–(3.50) become linearly dependent, providing only one condition.

3.4.3 Properties of Analytical Solution

In this section we investigate the properties of the functions $\Phi(\gamma, \mu)$ and $\Psi(\gamma, \nu)$, expressed by (3.55)–(3.56), when $0 \le \gamma \le 1$. Their schematic illustration is presented in Fig. 3.3. As γ increases from zero to unity, the function $\Phi(\gamma, \mu)$ decreases continuously and monotonically from 1 to 0, i.e.

$$1 \ge \Phi(\gamma, \mu) \ge 0, \quad \frac{\partial \Phi(\gamma, \mu)}{\partial \gamma} < 0, \quad 0 \le \gamma \le 1 \tag{3.64}$$

and

$$\Phi(0, \mu) = \left(\tanh\frac{\sqrt{1-\gamma}}{\mu}\,\coth\frac{\sqrt{1+\gamma}}{\mu}\right)_{\gamma=0} = 1 \tag{3.65}$$

$$\Phi(1, \mu) = \left(\tanh\frac{\sqrt{1-\gamma}}{\mu}\,\coth\frac{\sqrt{1+\gamma}}{\mu}\right)_{\gamma=1} = 0 \,. \tag{3.66}$$

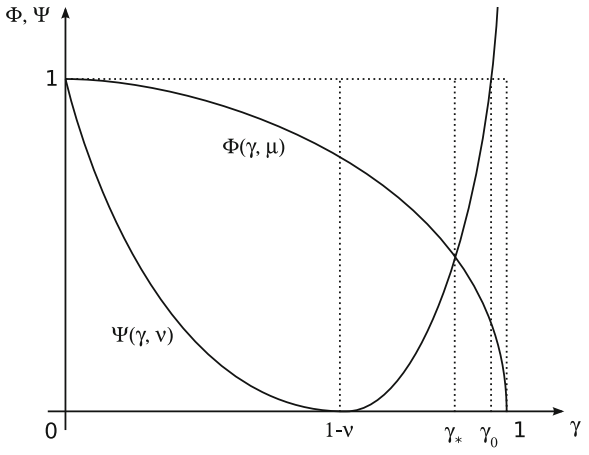

Fig. 3.3 Behavior of functions Φ and Ψ with respect to the parameter γ in the isotropic case. The presentation is qualitative

The proof of the monotonical decrease of function Φ is performed in Sect. 3.5.5, where we investigate the solution of the orthotropic problem. The same property for the present isotropic problem follows as a special case.

The function $\Psi\ (\gamma, \nu)$ decreases from 1 to 0 in the interval $0 < \gamma < 1 - \nu$,

$$1 > \Psi\ (\gamma, \nu) > 0, \quad \frac{\partial \Psi\ (\gamma, \nu)}{\partial \gamma} < 0, \quad 0 < \gamma < 1 - \nu\ , \tag{3.67}$$

and at the ends of this interval, we have

$$\Psi\ (0, \nu) = \left[\frac{\sqrt{1+\gamma}}{\sqrt{1-\gamma}} \frac{(\gamma + \nu - 1)^2}{(\gamma - \nu + 1)^2} \right]_{\gamma=0} = 1\ , \tag{3.68}$$

$$\Psi\ (1 - \nu, \nu) = \left[\frac{\sqrt{1+\gamma}}{\sqrt{1-\gamma}} \frac{(\gamma + \nu - 1)^2}{(\gamma - \nu + 1)^2} \right]_{\gamma=1-\nu} = 0\ . \tag{3.69}$$

The function Ψ increases monotonically in the interval $1 - \nu < \gamma < 1$, increasing without limit as $\gamma \to 1$, i.e.

$$0 < \Psi(\gamma, \nu) < \infty, \quad \frac{\partial \Psi(\gamma, \nu)}{\partial \gamma} > 0, \quad 1 - \nu < \gamma < 1 \tag{3.70}$$

and

$$\lim_{\gamma \to 1} \Psi\ (\gamma, \nu) = \infty\ . \tag{3.71}$$

The limit (3.71) will be shown in Sect. 3.5.5.

Plots of the function $\Phi(\gamma, \mu)$ when the geometric aspect ratio $\ell/2b = 0.1$, 1, and 10 are shown in Fig. 3.4 at the top. The functions $\Psi(\gamma, \nu)$ when $\nu = 0.2$, 0.3 and 0.5 are shown in the same figure, at the bottom.

The value of $\gamma = \gamma_0$, for which

$$\Psi(\gamma_0, \nu) = 1 \ , \quad \gamma_0 \in [1 - \nu, 1] \tag{3.72}$$

is of special interest. At this point it holds that

$$\Phi - \Psi = \Phi - \frac{1}{\Psi} \quad \text{at} \quad \gamma = \gamma_0 \ ,$$

and hence the functions defined by the left-hand sides of (3.54) and (3.59) will cross at the value $\gamma = \gamma_0$.

The value γ_0 is found by inserting (3.56) into (3.72), squaring both sides for convenience (we know that $\gamma_0 > 0$, so no information is lost), and solving for γ_0. We obtain

$$\gamma_0^2 = (1 - \nu)(3\nu - 1 + 2\sqrt{1 - 2\nu(1 - \nu)}) \ . \tag{3.73}$$

The other solutions are all negative and can thus be discarded. When examined as a function of ν, the expression $\gamma_0(\nu)$ has zeros at $\nu = -3$ and $\nu = 1$, and a maximum at $\nu = 0$, with the value $\gamma_0 = 1$. For any other value of ν, we have $\gamma_0 < 1$.

If we restrict the Poisson ratio ν into the physically admissible range for isotropic materials, $\nu \in (-1, 0.5)$, then the value of γ_0, as given by (3.73), turns out to be close to unity. The minimal values are encountered at the ends of the range. At $\nu = -1$ we have $\gamma_0 \approx 0.944$, and at $\nu = 0.5$, $\gamma_0 \approx 0.957$.

Let us consider the limiting cases in terms of the band geometry. First, if we have a long and narrow band span, $\ell \gg b$, the geometric parameter μ becomes large, and the arguments of tanh and coth in (3.55) become small. In such a case, we can use the following Taylor series expansions of the hyperbolic trigonometrics around $\alpha = 0$ (here α is an arbitrary parameter):

$$\begin{aligned} \tanh \alpha &= \alpha - \frac{1}{3}\alpha^3 + \frac{2}{15}\alpha^5 + \dots \ , \\ \coth \alpha &= \frac{1}{\alpha} + \frac{1}{3}\alpha - \frac{1}{45}\alpha^3 + \dots \ . \end{aligned} \tag{3.74}$$

Retaining only the first term in each of (3.74), and applying to (3.55), we obtain the approximate expression

$$\Phi = \sqrt{\frac{1 - \gamma}{1 + \gamma}} \qquad \text{(for large } \mu) \ . \tag{3.75}$$

Using (3.75) and (3.56) in (3.54), we find the solution

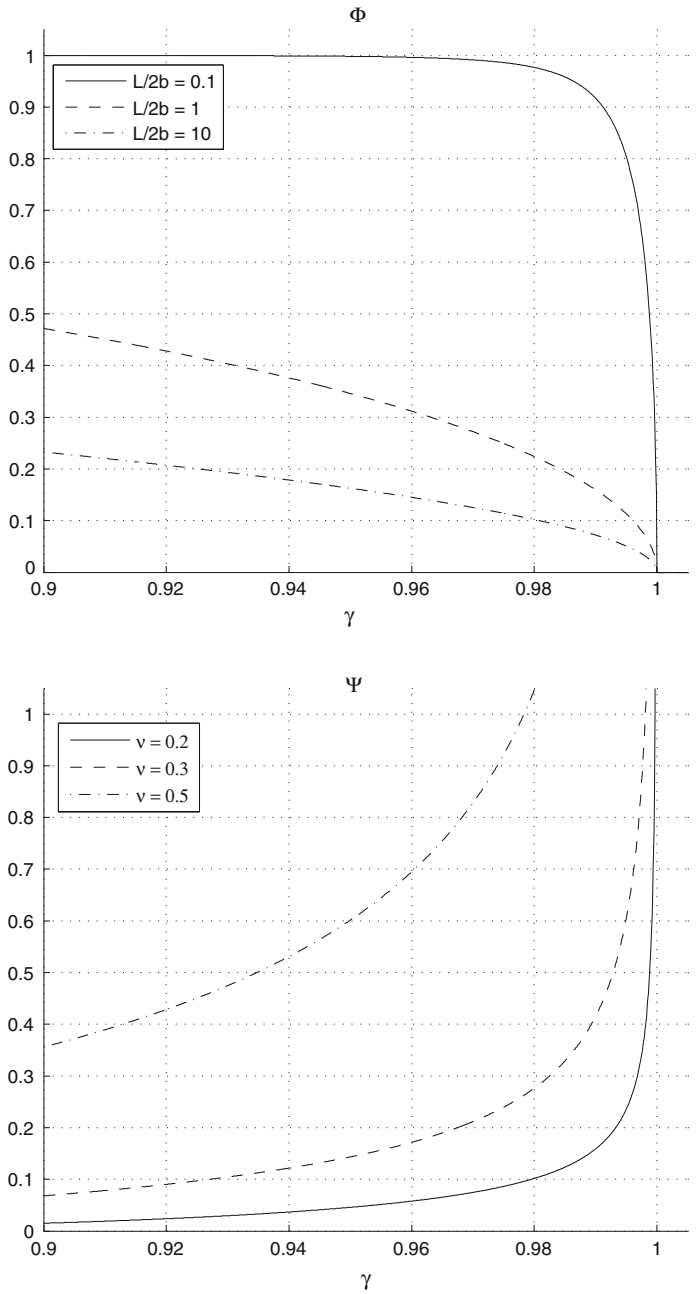

Fig. 3.4 Plots of Φ (*top*) and Ψ (*bottom*) for different values of the parameters $\ell/2b$ and ν. Note the horizontal scale

$$\lambda_e = \gamma_e^2 = 1 - \nu^2 \ . \tag{3.76}$$

This solution corresponds to a narrow strip simply supported at its ends. It leads to the Euler value of the force for stability loss (buckling),

$$P = P_e = \lambda_e \frac{\pi^2 D}{\ell^2} = \pi^2 \frac{EI}{\ell^2} \ , \tag{3.77}$$

where

$$P = mV_0^2 - T_0 \ , \quad D = \frac{Eh^3}{12(1-\nu^2)} \ , \quad I = \frac{h^3}{12} \ . \tag{3.78}$$

Furthermore, consider the Taylor expansion of $\cosh\alpha$ around $\alpha = 0$ (here also α is an arbitrary parameter):

$$\cosh\alpha = 1 + \frac{1}{2}\alpha^2 + \frac{1}{24}\alpha^4 + \dots \ .$$

Retaining only the first term, we have a constant value. Looking at (3.47), which determines the corresponding mode of stability loss, we see that for large μ, the dependence on η thus vanishes, making the mode cylindrical.

With regard to both the critical load and the mode, we see that the case of a long, narrow strip corresponds to the classical one-dimensional case.

At the other extreme, for a very wide band for which $b \gg \ell$, we have $\mu \to 0$. In this case, we can use the limits

$$\begin{aligned} &\lim_{\alpha\to\infty} \tanh\alpha = 1 \ , \\ &\lim_{\alpha\to\infty} \coth\alpha = 1 \ , \end{aligned} \tag{3.79}$$

leading to

$$\lim_{\mu\to 0^+} \Phi(\gamma, \mu) = 1 \ . \tag{3.80}$$

Using (3.80) and (3.56) in (3.54), we obtain the equation $\Psi(\gamma, \nu) = 1$ at the limit $\mu \to 0$. Its solution is $\gamma = \gamma_0$, given by (3.73) above. Thus, if $\nu \neq 0$, it holds for the wide band that

$$\gamma_* \to \gamma_0 \neq 1 \quad \text{for} \quad \mu \to 0 \ , \tag{3.81}$$

which differs from the classical one-dimensional value $\gamma_e = \sqrt{1-\nu^2}$ given by (3.76). Numerically, it is seen that $\gamma_0 \geq \gamma_e$ for all $\nu \in (-1, 0.5)$, where the equality holds only at $\nu = 0$. Thus, the minimal eigenvalue in the limit of a wide band is almost always higher than the minimal eigenvalue of the classical one-dimensional case.

It also turns out that the corresponding mode of stability loss from (3.46)–(3.48) is not cylindrical. It is therefore seen that the case of a wide band does not reduce to the classical one-dimensional case.

For naturally occurring materials, for which $\nu \geq 0$, the largest difference between the critical parameter γ_*, which leads to the loss of stability of an infinitely wide band, and the corresponding value obtained assuming a distribution of the deflections in the form of cylindrical surface, occurs when $\nu = 0.5$, i.e., in the case of an absolutely incompressible material. For auxetic materials, for which $\nu < 0$, the largest difference occurs at the lower limit of the range, i.e. $\nu = -1$.

It follows from the above treatment and the properties of the functions $\Phi(\gamma, \mu)$ and $\Psi(\gamma, \nu)$ that the roots $\gamma = \gamma_*$ of (3.54) lie in the interval

$$\gamma_e \leq \gamma_* \leq \gamma_0 \tag{3.82}$$

for all $0 < \mu < \infty$. This is the property that is needed to complete the analysis of (3.62).

Some numerical examples of the divergence velocities, V_0^{div}, defined in (3.63), and the corresponding buckling modes will be given. The used values of physical parameters are given in Table 3.1. These parameters represent typical values of paper material and conditions of paper making.

Figure 3.5 shows some examples of the critical buckling modes (divergence modes), calculated with the help of relations in (3.46)–(3.48), (3.49) and (3.54)–(3.56), for different values of the aspect ratio $\ell/(2b)$. We see a localisation phenomenon: most of the displacement in the buckling mode occurs near the free edges. This effect becomes more pronounced as the width of the plate increases with respect to its length.

Table 3.2 presents some example values of critical velocities V_0^{div} of an axially moving isotropic plate. The row with $\nu = 0.3$ corresponds to the plots in Fig. 3.5.

3.5 Divergence Instability of Orthotropic Plates

The ratio of Young's moduli, i.e. the degree of orthotropicity, defines the properties of the actual paper product, affecting its behaviour. Different degrees of orthotropicity are desired for different applications. Using an orthotropic material model, we can bring the analysis closer to the real life situation that is being modelled.

In this section, we will extend the results from Sect. 3.4 into the case of orthotropic materials.

Table 3.1 Physical parameters used in the numerical examples

T_0	m	h	E
500 N/m	0.08 kg/m^2	10^{-4} m	10^9 N/m^2

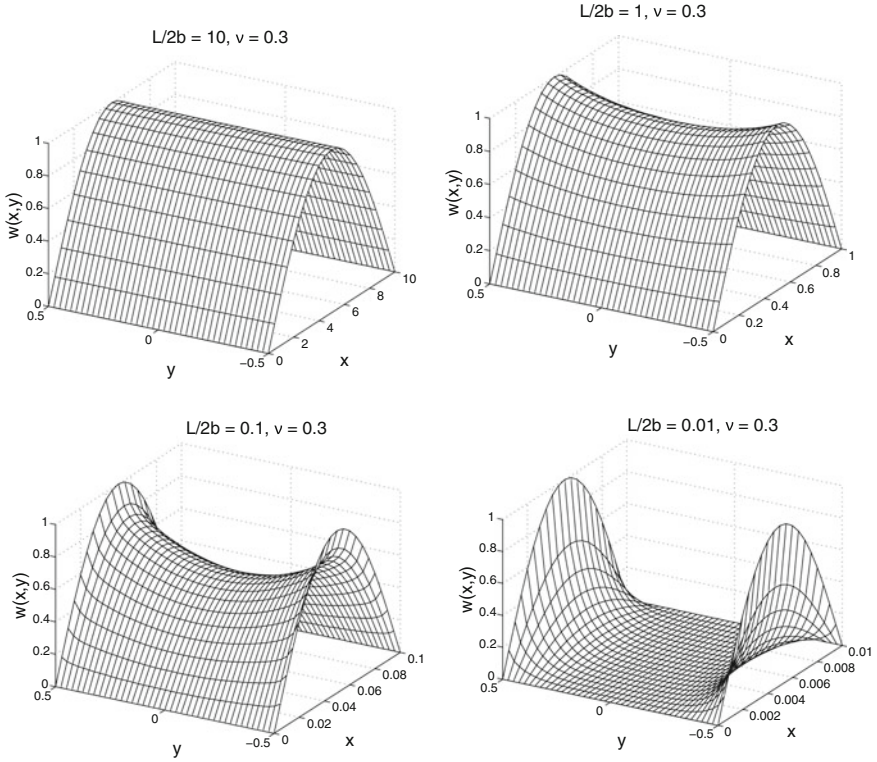

Fig. 3.5 Critical buckling modes (divergence modes) of an axially moving isotropic plate. Localization of deflections in the vicinity of the free boundaries can be seen, with the effect growing stronger as the aspect ratio $\ell/2b$ is decreased. (Reproduced from Banichuk et al. 2010a)

Table 3.2 Critical velocities, i.e. divergence velocities V_0^{div} (m/s) of an axially moving isotropic plate for selected values of Poisson ratio ν and the span length ℓ

ν	ℓ (m)			
	10	1	0.1	0.01
0.1	79.0569	79.0570	79.0635	79.7110
0.3	79.0569	79.0570	79.0640	79.7659
0.5	79.0569	79.0570	79.0652	79.8824

The width of the plate is $2b = 1$ m in all cases. The other physical parameters used are given in Table 3.1. (Banichuk et al. 2010a)

3.5.1 Eigenvalue Problem

The problem is formulated similarly to the isotropic eigenvalue problem, but now describing the divergence (static instability) of the travelling orthotropic plate subjected to homogeneous tension. We have the partial differential equation

$$\left(mV_0^2 - T_0\right)\frac{\partial^2 W}{\partial x^2} + D_0\mathcal{L}_0(W) = 0\ , \tag{3.83}$$

with the boundary conditions (3.16)–(3.18); see Sect. 3.3.2. Here the bending operator $\mathcal{L}_0(W)$ is

$$\mathcal{L}_0(W) = \frac{D_1}{D_0}\frac{\partial^4 W}{\partial x^4} + \frac{2D_3}{D_0}\frac{\partial^4 W}{\partial x^2 \partial y^2} + \frac{D_2}{D_0}\frac{\partial^4 W}{\partial y^4}\ , \tag{3.84}$$

where the coefficients D_j for $j = 1, 2, 3$ are the orthotropic bending rigidities

$$D_1 = \frac{h^3}{12}C_{11}\ , \quad D_2 = \frac{h^3}{12}C_{22}\ , \quad D_3 = \frac{h^3}{12}\left(C_{12} + 2\,C_{66}\right)\ ,$$

which were already introduced as (2.18), Sect. 2.1.3 (or see Timoshenko and Woinowsky-Krieger 1959, Chap. 11). The C_{ij} are the elastic moduli, (2.19). In (3.83) and (3.84), the coefficient D_0 is an arbitrary constant, which is convenient to take as $D_0 = D_1$.

We wish to determine the minimal eigenvalue,

$$\lambda = \gamma^2 = \frac{\ell^2}{\pi^2 D_0}\left(mV_0^2 - T_0\right)\ , \tag{3.85}$$

of the problem (3.16)–(3.18) and (3.83)–(3.84). For the corresponding eigenfunction $W = W(x, y)$, we apply the same representation as before,

$$W = W\,(x, y) = f\left(\frac{y}{b}\right)\sin\left(\frac{\pi x}{\ell}\right)\ . \tag{3.86}$$

As was noted, the fact that the solution is a half-sine in the longitudinal direction is well-known in the isotropic case. It can be shown that the same form is applicable for the orthotropic plate. Again, what remains to be determined is the unknown cross-section $f\,(y/b)$.

It follows from (3.86) that the desired buckling form W (steady-state solution) satisfies the boundary condition (3.16). Using the dimensionless quantities (same as before in Sect. 3.4)

$$\eta = \frac{y}{b}\ , \quad \mu = \frac{\ell}{\pi b}\ , \tag{3.87}$$

and the relations (3.17)–(3.18) and (3.83)–(3.86), we obtain the following eigenvalue problem for the unknown function $f(\eta)$:

$$\mu^4 H_2 \frac{\mathrm{d}^4 f}{\mathrm{d}\eta^4} - 2\mu^2 H_3 \frac{\mathrm{d}^2 f}{\mathrm{d}\eta^2} + (H_1 - \lambda)\, f = 0\,, \qquad -1 < \eta < 1\,, \tag{3.88}$$

$$\mu^2 \frac{\mathrm{d}^2 f}{\mathrm{d}\eta^2} - \beta_1 f = 0\,, \qquad \eta = \pm 1\,, \tag{3.89}$$

$$\mu^2 \frac{\mathrm{d}^3 f}{\mathrm{d}\eta^3} - \beta_2 \frac{\mathrm{d} f}{\mathrm{d}\eta} = 0\,, \qquad \eta = \pm 1\,, \tag{3.90}$$

where H_1, H_2 and H_3 are dimensionless bending rigidities, defined by

$$H_1 = \frac{D_1}{D_0}\,, \qquad H_2 = \frac{D_2}{D_0}\,, \qquad H_3 = \frac{D_3}{D_0}\,, \tag{3.91}$$

and D_0 is the characteristic bending rigidity, which is an arbitrary constant. In this book, we will use the choice $D_0 = D_1$, which will be convenient in the calculations to follow. The parameters β_1 and β_2 are given by (3.19). Equations (3.89)–(3.90) represent the free-of-traction boundary conditions.

3.5.2 Non-Negativeness of Eigenvalues

To show that the eigenvalues λ of the problem (3.88)–(3.90) are non-negative, one can proceed by using general ideas from Chen et al. (1998), who proved a similar result for an isotropic stationary plate. Let us denote

$$\mathcal{L}_1(f) = \mu^4 H_2 \frac{\mathrm{d}^4 f}{\mathrm{d}\eta^4} - 2\,\mu^2 H_3 \frac{\mathrm{d}^2 f}{\mathrm{d}\eta^2} + H_1 f\,. \tag{3.92}$$

We introduce the bilinear form $a\,(f, g)$ that corresponds to the strain energy of a plate (see e.g. Timoshenko and Woinowsky-Krieger 1959),

$$\begin{aligned} a\,(f, g) = \int_{-1}^{1} \Bigg[& H_1 f\, \bar{g} - \mu^2 B_1 f\, \frac{\mathrm{d}^2 \bar{g}}{\mathrm{d}\eta^2} - \mu^2 B_1 \frac{\mathrm{d}^2 f}{\mathrm{d}\eta^2}\, \bar{g} \\ & + \mu^4 H_2 \frac{\mathrm{d}^2 f}{\mathrm{d}\eta^2} \frac{\mathrm{d}^2 \bar{g}}{\mathrm{d}\eta^2} + 4\mu^2 B_2 \frac{\mathrm{d} f}{\mathrm{d}\eta} \frac{\mathrm{d}\bar{g}}{\mathrm{d}\eta} \Bigg] \mathrm{d}\eta\,, \end{aligned} \tag{3.93}$$

where

$$B_1 + 2\,B_2 = H_3\,, \tag{3.94}$$

and $\bar{g}$ denotes the complex conjugate of g. Performing integration by parts on the bilinear form (3.93), we obtain

$$a\,(f,g) = \int_{-1}^{1}\left[\mu^4 H_2 \frac{\mathrm{d}^4 f}{\mathrm{d}\eta^4} - 2\,\mu^2 H_3 \frac{\mathrm{d}^2 f}{\mathrm{d}\eta^2} + H_1 f\right]\bar{g}\,\mathrm{d}\eta\ . \tag{3.95}$$

Thus, the form $a(f, g)$ can alternatively be defined as

$$a\,(f,g) \;=\; (\mathcal{L}_1\,(f)\,,g)\ , \tag{3.96}$$

where the inner product $(\cdot\,,\cdot\,)$ is

$$(u,v) \;=\; \int_{-1}^{1} u\,\bar{v}\,\mathrm{d}\eta\ , \tag{3.97}$$

for arbitrary functions u and v. The operator $\mathcal{L}_1(f)$ is self-adjoint, and the form $a(f, g)$ induces a positive semidefinite norm $a(f, f)$:

$$\begin{aligned} a(f,f) = \int_{-1}^{1}\Bigg[& H_1\left\| f - \mu^2 \nu_{21}\frac{\mathrm{d}^2 f}{\mathrm{d}\eta^2}\right\|^2 + \mu^4 H_2(1-\nu_{12}\nu_{21})\left\|\frac{\mathrm{d}^2 f}{\mathrm{d}\eta^2}\right\|^2 \\ & + 4\,\mu^2 B_2\left\|\frac{\mathrm{d}f}{\mathrm{d}\eta}\right\|^2\Bigg]\mathrm{d}\eta \;\geq 0\ . \end{aligned} \tag{3.98}$$

This implies that the eigenvalues of $\mathcal{L}_1(f)$ are nonnegative. That is,

$$\lambda \geq 0 \tag{3.99}$$

for all eigenvalues λ of the problem (3.88)–(3.90), which governs the cross-sectional eigenfunctions $f(y)$ and the corresponding eigenvalues of the buckled, travelling orthotropic plate.

3.5.3 Analytical Solution

The general solutions of the ordinary differential equation (3.88) have the form

$$f = Ae^{p\eta}\ , \qquad p = \frac{\kappa}{\mu}\ , \tag{3.100}$$

where A is an arbitrary constant and κ is a solution of the following biquadratic algebraic characteristic equation:

$$H_2\kappa^4 - 2H_3\kappa^2 + (H_1 - \lambda) = 0\ . \tag{3.101}$$

The solution can be written as

$$\kappa_{\pm}^2 = \frac{H_3}{H_2}\left(1 \pm \sqrt{1 - \frac{H_2(H_1 - \lambda)}{H_3^2}}\right) = \frac{H_3}{H_2}\left(1 \pm \sqrt{1 - \frac{H_2(1 - \lambda)}{H_3^2}}\right) , \quad (3.102)$$

where the upper, and respectively the lower, signs correspond to each other. In the last form on the right, we have used the choice $D_0 = D_1$, which leads to $H_1 = 1$.

Let us consider the range of λ where the solution is real-valued. The numbers $\kappa_{\pm}^2$ are real-valued if the expression under the square root in (3.102) is nonnegative. This implies the following lower limit for λ:

$$\lambda_{\mathrm{m}} \equiv 1 - \frac{H_3^2}{H_2} < \lambda , \quad (3.103)$$

corresponding to a real-valued eigenfunction f. Note that in the case $\lambda = \lambda_{\mathrm{m}}$, the solution of (3.101) is

$$\kappa = \pm\sqrt{\frac{H_3}{H_2}} , \quad (3.104)$$

where both solutions are double roots.

Furthermore, if we require not only $\kappa_{\pm}^2$, but also $\kappa_{\pm}$ to be real-valued, the whole parenthetical expression in (3.102) must then be nonnegative. This gives us an upper limit for λ:

$$\lambda \leq 1 \equiv \lambda_{\max} . \quad (3.105)$$

Equation (3.105) holds regardless of the values of the problem parameters.

For the lower limit given by (3.103), it holds that

$$\lambda_{\mathrm{m}} \leq 0 \quad \text{when} \quad G_{12} \geq G_{\mathrm{H}} , \quad (3.106)$$

where G_{12} is the in-plane shear modulus of the orthotropic material (which is considered an independent material parameter), and G_{H} is the geometric average shear modulus. The quantity G_{H} is given by (2.25), repeated here for convenience:

$$G_{\mathrm{H}} \equiv \frac{\sqrt{E_1 E_2}}{2\left(1 + \sqrt{\nu_{12}\nu_{21}}\right)} . \quad (3.107)$$

By (3.99) and (3.103)–(3.105), in the case that (3.106) holds, we may seek the lowest eigenvalue in the range $0 \leq \lambda \leq 1$, as was done in the isotropic case in Sect. 3.4.

On the other hand, one can find examples of measurements of G_{12} for paper materials, which indicate $G_{12} < G_{\mathrm{H}}$. See, e.g., the articles of Mann et al. (1980), Seo (1999), Yokoyama and Nakai (2007), and Bonnin et al. (2000). For such a material,

$$\lambda_{\mathrm{m}} > 0 \quad \text{when} \quad G_{12} < G_{\mathrm{H}} . \quad (3.108)$$

This will produce complex solutions $\kappa_\pm$ and complex eigenfunctions if λ is between zero and λ_m. In practice however, it has been numerically observed (from (3.115), presented further below) that this interval contains no solutions. Thus, in this case the search for the lowest eigenvalue can be performed in the range $\lambda_\mathrm{m} \leq \lambda \leq 1$.

These considerations motivate the definition

$$\lambda_{\min} \equiv \max\left(\lambda_\mathrm{m}, 0\right) \ , \tag{3.109}$$

enabling us to define the relevant range for solutions as

$$\lambda_{\min} \leq \lambda \leq \lambda_{\max} \tag{3.110}$$

regardless of the value of the shear modulus G_{12}. The quantities λ_m and $\lambda_{\max}$ are defined by (3.103) and (3.105), respectively.

From (3.100) and (3.102) in the case that $\lambda \neq \lambda_\mathrm{m}$, we obtain that the general solution can be represented in the form

$$f(\eta) = A_1 e^{+\frac{\kappa_+ \eta}{\mu}} + A_2 e^{-\frac{\kappa_+ \eta}{\mu}} + A_3 e^{+\frac{\kappa_- \eta}{\mu}} + A_4 e^{-\frac{\kappa_- \eta}{\mu}} \tag{3.111}$$

with unknown constants A_1, A_2, A_3 and A_4.

The eigenvalue boundary value problem (3.88)–(3.90) is invariant under the symmetry operation $\eta \to -\eta$, and consequently the eigenforms can be classified into functions that are symmetric (f^s) or antisymmetric (f^a) with respect to the origin. Using the relations (3.88)–(3.90) and (3.111), we obtain a general representation for the function $f^\mathrm{s}(\eta)$ and linear algebraic equations for determining the constants A^s and B^s:

$$f^\mathrm{s}(\eta) = A^\mathrm{s} \cosh\frac{\kappa_+ \eta}{\mu} + B^\mathrm{s} \cosh\frac{\kappa_- \eta}{\mu} \ , \tag{3.112}$$

$$A^\mathrm{s}\left(\kappa_+^2 - \beta_1\right)\cosh\frac{\kappa_+}{\mu} + B^\mathrm{s}\left(\kappa_-^2 - \beta_1\right)\cosh\frac{\kappa_-}{\mu} = 0 \ , \tag{3.113}$$

$$A^\mathrm{s}\kappa_+\left(\kappa_+^2 - \beta_2\right)\sinh\frac{\kappa_+}{\mu} + B^\mathrm{s}\kappa_-\left(\kappa_-^2 - \beta_2\right)\sinh\frac{\kappa_-}{\mu} = 0 \ , \tag{3.114}$$

where A^s and B^s are unknown constants. Due to the symmetry (or antisymmetry) of the solution f, we have only two independent unknown constants, instead of the four in the general representation (3.111), where the symmetry considerations had not yet been applied.

Proceeding in the same manner as in the isotropic case of Sect. 3.4.2, the conditions for a non-trivial solution to exist in the form of (3.112)–(3.114) reduce to the requirement that the determinant of the homogeneous linear system (3.113)–(3.114) vanishes.

Again, at the solution point, the zero determinant condition leads to the linear dependence of the equations (3.113)–(3.114), providing only one independent con-

dition. Thus, we may solve either of (3.113)–(3.114) for either A^{s} or B^{s}, and choose the other (free) coefficient arbitrarily.

After rearrangement, the zero determinant condition can be expressed in the convenient form

$$\Phi(\gamma, \mu, \nu_{12}, E_1, E_2, G_{12}) - \Psi(\gamma, \nu_{12}, E_1, E_2, G_{12}) = 0 \,, \tag{3.115}$$

where

$$\Phi(\gamma, \mu, \nu_{12}, E_1, E_2, G_{12}) = \tanh \frac{\kappa_-}{\mu} \coth \frac{\kappa_+}{\mu} \,, \tag{3.116}$$

$$\Psi(\gamma, \nu_{12}, E_1, E_2, G_{12}) = \frac{\kappa_+(\kappa_+^2 - \beta_2)(\kappa_-^2 - \beta_1)}{\kappa_-(\kappa_+^2 - \beta_1)(\kappa_-^2 - \beta_2)} \,, \tag{3.117}$$

and

$$\kappa_+ = \kappa_+(\gamma, \nu_{12}, E_1, E_2, G_{12}) \,, \qquad \kappa_- = \kappa_-(\gamma, \nu_{12}, E_1, E_2, G_{12}) \,. \tag{3.118}$$

The obtained transcendental equation (3.115) can be used to determine the eigenvalues

$$\lambda = \gamma^2 \tag{3.119}$$

corresponding to symmetric eigenfunctions with different values of the parameters μ, ν_{12}, E_1, E_2 and G_{12}.

In the definitions of Φ and Ψ, (3.116)–(3.117), there is no dependence on the parameter ν_{21}, because it depends on ν_{12}, E_1 and E_2 via the compatibility relation (2.36). The independent parameters in Φ and Ψ can be chosen also in a different way, by choosing any combination of exactly three parameters out of E_1, E_2, ν_{12} and ν_{21}. Relation (2.36) can then be used to eliminate the remaining parameter.

Similarly, using the relations (3.89) and (3.90), we can obtain a representation for antisymmetric eigenfunctions $f^{\mathrm{a}}(\eta)$, the equation for determining the corresponding constants A^{a} and B^{a}, and the transcendental equation

$$\Phi - \frac{1}{\Psi} = 0 \,, \tag{3.120}$$

where Φ and Ψ are the functions defined in (3.116)–(3.117). These equations can be used for determining the eigenvalues corresponding to antisymmetric eigenforms. The representations differ from (3.112)–(3.114) through the replacements

$$\cosh \to \sinh \quad \text{and} \quad \sinh \to \cosh \,. \tag{3.121}$$

Again, it turns out that the minimal antisymmetric eigenvalue is higher than the minimal symmetric one, so we will only consider the symmetric case.

In the special case that $\lambda = \lambda_m$, the characteristic equation (3.101) has two double roots (3.104), and then, the general solution has the form

$$f(\eta) = A_1 e^{+\frac{\kappa\eta}{\mu}} + A_2 e^{-\frac{\kappa\eta}{\mu}} + A_3 \eta e^{+\frac{\kappa\eta}{\mu}} + A_4 \eta e^{-\frac{\kappa\eta}{\mu}} .$$

In this case, the symmetric solution has the form

$$f^s(\eta) = A^s \cosh\frac{\kappa\eta}{\mu} + B^s \eta \sinh\frac{\kappa\eta}{\mu} . \tag{3.122}$$

For this solution, we will also have a zero determinant condition (different from (3.115) and (3.120)) but for a fixed κ. It can be calculated that the determinant condition does not hold for (3.122) with the boundary conditions (3.89)–(3.90), and thus, there is no symmetric solution of the form (3.122), and we will have no solution when $\lambda = \lambda_m$. The antisymmetric case can be explored in a similar manner.

Similar remarks about finalizing the solution apply as in Sect. 3.4.2. Once (3.115) has been solved, obtaining the minimal symmetric eigenvalue γ_*, the corresponding critical velocity of the travelling orthotropic plate can be found from (3.85). The critical velocity is

$$(V_0^{\text{div}})^2 = \frac{T_0}{m} + \frac{\gamma_*^2}{m}\left(\frac{\pi^2 D_0}{\ell^2}\right) . \tag{3.123}$$

Then, in order to obtain the corresponding eigenmode, we can solve for either A^s or B^s, picking either of the equations (3.113)–(3.114). Recall that the equations are linearly dependent at the solution point $\gamma = \gamma_*$, so it does not matter which one is used. The other coefficient (either B^s or A^s, respectively) is then the free coefficient of the eigenvalue problem, and can be assigned an arbitrary value. Finally, inserting the obtained γ_*, A^s and B^s into (3.86), (3.102) and (3.112) gives the eigenmode corresponding to the eigenvalue γ_*.

3.5.4 Properties of Analytical Solution

In this section, we will investigate the properties of the functions Φ and Ψ, when λ is in the range $\lambda_m \leq \lambda \leq 1$, where λ_m is given by (3.103).

Unlike in the isotropic case described in Sect. 3.4.3, the decoupling between the geometric and material parameters is very minimal. The function Ψ does not depend on the aspect ratio μ (plate geometry), but both Φ and Ψ depend on all independent material parameters (ν_{12}, E_1, E_2 and G_{12}).

We start our examination by noting that (by direct calculation)

$$\Phi(\lambda_{\mathrm{m}}) = 1 \,, \tag{3.124}$$

$$\Psi(\lambda_{\mathrm{m}}) = 1 \,, \tag{3.125}$$

and

$$\Phi(1) = 0 \,, \tag{3.126}$$

regardless of the problem parameters. We defer the evaluation of

$$\lim_{\lambda \to \lambda_{\max}} \Psi(\lambda) \tag{3.127}$$

to Sect. 3.5.5. Although it is trivial to see that Ψ has a singularity there, because $\kappa_- \to 0^+$ as $\lambda \to \lambda_{\max}$, in order to deduce the sign of the singularity we need to know the sign of each of the terms in (3.117).

Let us assume the values of ν_{12}, E_1, E_2 and G_{12} to be given and that they correspond to some orthotropic material. The qualitative behavior of the functions Φ and Ψ is illustrated in Fig. 3.6. Recall that the corresponding isotropic case was illustrated further above, Fig. 3.3 in Sect. 3.4.

The range for γ, which is defined in (3.85), is obtained by taking the square root of each side of the inequality in (3.110). Note that the x axis in Fig. 3.3 starts at

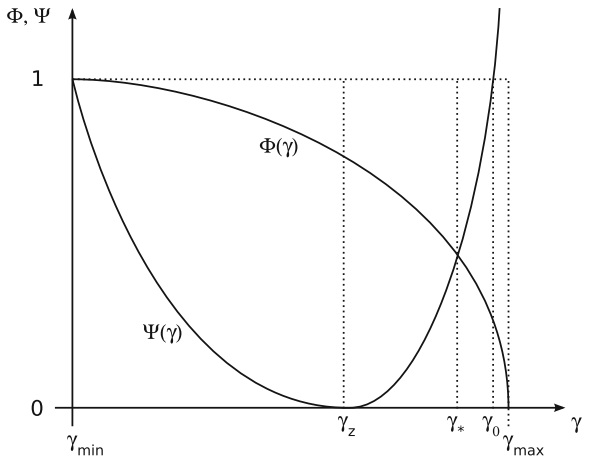

Fig. 3.6 Behaviour of Φ and Ψ in the orthotropic case, as a function of γ, when the parameters D_1, D_2, D_3, μ, β_1 and β_2 are fixed. This is a qualitative drawing illustrating the case $G_{12} \leq G_{\mathrm{H}}$ (for which $\gamma_{\min} = \gamma_{\mathrm{m}}$). The main difference between this figure and Fig. 3.3 is that on the x axis, the functions begin at $\gamma_{\min}$ instead of 0, and the location of the zero of the function Ψ is γ_{z} instead of $1 - \nu$. (Reproduced from Banichuk et al. 2011a)

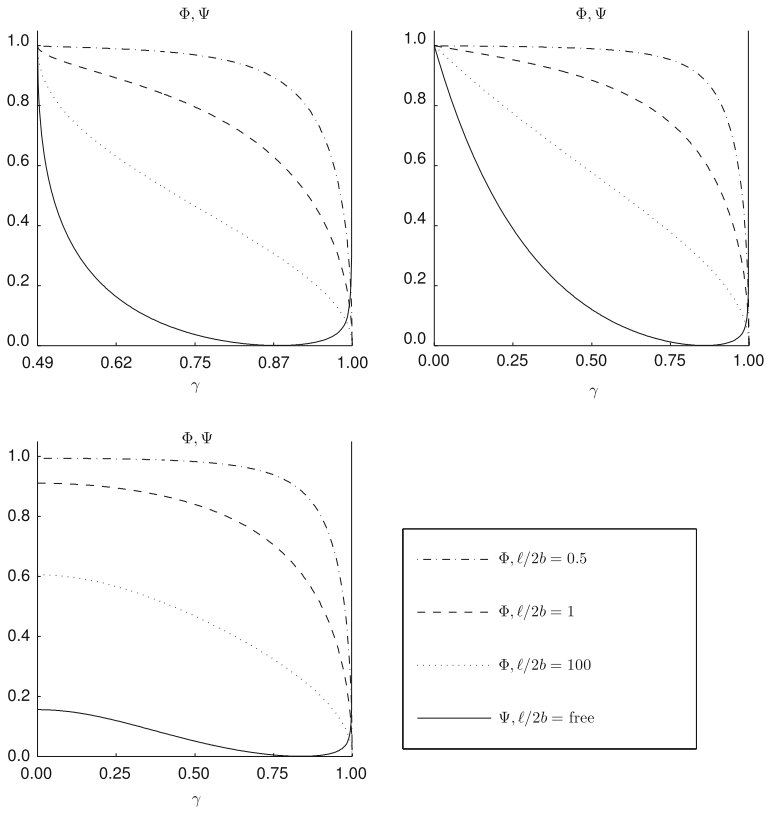

Fig. 3.7 Behaviour of functions Φ and Ψ for some orthotropic materials, at different aspect ratios $\ell/2b$ and different values for the in-plane shear modulus G_{12}. For all cases, the other material parameters are $E_1 = 6.8$ GPa, $E_2 = 3.4$ GPa and $\nu_{12} = 0.2$, $\nu_{21} = 0.1$. Note that only Φ depends on the aspect ratio. *Upper left* $G_{12} = 0.85\ G_{\mathrm{H}}$ (note the scale for γ). *Upper right* $G_{12} = G_{\mathrm{H}}$. *Lower left* $G_{12} = 1.15\ G_{\mathrm{H}}$, where G_{H} is the geometric average shear modulus (3.107). The range of γ is $\gamma_{\min} \leq \gamma \leq \gamma_{\max}$, based on (3.85) and (3.110), and evaluated separately for each subfigure. Observe that for the *lower right* subfigure, $\gamma_{\min} = 0 > \gamma_{\mathrm{m}}$, causing the qualitative behaviour of the functions to differ from the other cases where $\gamma_{\min} = \gamma_{\mathrm{m}}$. (Reproduced from Banichuk et al. 2011a)

$\gamma_{\min}$. In the isotropic case, we had $\gamma_{\min} = 0$, which does not hold in general for the orthotropic case.

Figure 3.7 shows some examples of Φ and Ψ plotted for some orthotropic materials. As discussed above, only Φ depends on the aspect ratio $\ell/2b$. We see that the case $G_{12} = G_{\mathrm{H}}$ behaves like the isotropic case, as expected (compare with Sect. 3.4.3). When the value of G_{12} deviates from the geometric average shear modulus (3.107), it is seen that when $G_{12} < G_{\mathrm{H}}$, the curvature of Φ becomes more pronounced, especially for a large aspect ratio. If $G_{12} > G_{\mathrm{H}}$, the value of both functions at $\gamma = \gamma_{\min}$

decreases (because then $\gamma_{\min} = 0 > \gamma_{\mathrm{m}}$), again especially for a large aspect ratio in the case of Φ.

When γ increases from γ_{m} to $\gamma_{\max}$, the function $\Phi(\gamma, \mu)$ decreases continuously and monotonically from 1 to 0, i.e.

$$1 \geq \Phi(\gamma, \mu) \geq 0 \,, \qquad \frac{\partial \Phi(\gamma, \mu)}{\partial \gamma} < 0 \,, \qquad \gamma_{\mathrm{m}} \leq \gamma \leq \gamma_{\max} \,. \tag{3.128}$$

The critical values of the function Φ in that interval are

$$\Phi(\gamma_{\mathrm{m}}, \mu) = \left(\tanh \frac{\kappa -}{\mu} \coth \frac{\kappa_+}{\mu} \right)_{\gamma = \gamma_{\mathrm{m}}} = 1 \tag{3.129}$$

and

$$\Phi(\gamma_{\max}, \mu) = \left(\tanh \frac{\kappa -}{\mu} \coth \frac{\kappa_+}{\mu} \right)_{\gamma = \gamma_{\max}} = 0 \,. \tag{3.130}$$

The function $\Psi(\gamma)$ decreases monotonically from 1 to 0 in the interval $\gamma_{\mathrm{m}} < \gamma < \gamma_{\mathrm{z}}$:

$$1 > \Psi(\gamma) > 0 \,, \qquad \frac{\partial \Psi(\gamma)}{\partial \gamma} < 0 \,. \tag{3.131}$$

The values of the function Ψ at the ends of the interval are

$$\Psi(\gamma_{\mathrm{m}}) = 1 \tag{3.132}$$

and

$$\Psi(\gamma_{\mathrm{z}}) = 0 \,. \tag{3.133}$$

The function Ψ increases monotonically in the interval $\gamma_{\mathrm{z}} < \gamma < \gamma_{\max}$, increasing without limit when $\gamma \to \gamma_{\max}$:

$$0 < \Psi(\gamma) < \infty \,, \qquad \frac{\partial \Psi(\gamma)}{\partial \gamma} > 0 \,, \tag{3.134}$$

Thus at the ends of the interval, the values of Ψ are

$$\Psi(\gamma_{\mathrm{z}}) = 0 \,,$$

and

$$\lim_{\gamma \to \gamma_{\max}} \Psi(\gamma) = \infty \,.$$

The function touches zero at the point

$$\gamma_{\mathrm{z}} = \sqrt{\beta_j^2 H_2 - 2\beta_j H_3 + H_1} \,, \tag{3.135}$$

where $j = 1, 2$. It will be shown below that γ_z is unique. Thus either choice for j results in the same value for γ_z.

Because

$$0 \leq \Phi \leq 1 \qquad \text{for all} \qquad \gamma_{\min} \leq \gamma \leq \gamma_{\max} \tag{3.136}$$

the symmetric solution in (3.115) is only possible in the range where $\Psi \leq 1$. Likewise, the antisymmetric solution in (3.120) is only possible in the range where

$$\frac{1}{\Psi} \leq 1 \qquad \text{i.e.} \qquad \Psi \geq 1 \,. \tag{3.137}$$

Again, at the point $\gamma = \gamma_0$ for which $\Psi = 1$, it also holds that $1/\Psi = 1$, and thus at this point we have

$$\Phi - \Psi = \Phi - \frac{1}{\Psi} \quad \text{at} \quad \gamma = \gamma_0 \,. \tag{3.138}$$

That is, the functions defined by the left-hand sides of (3.115) and (3.120) will cross at the value $\gamma = \gamma_0$.

Equation (3.131), combined with the consideration in the previous paragraph, implies that the eigenvalue γ_* corresponding to the symmetric solution is always lower than the eigenvalues γ_1 and γ_2 corresponding to the antisymmetric solution. Additionally, since

$$\Phi(\gamma_{\max}, \mu) = 0 \qquad \text{and} \qquad \lim_{\gamma \to \gamma_{\max}} \Psi(\gamma) = \infty \,, \tag{3.139}$$

we see that the second antisymmetric eigenvalue must be $\gamma_2 = \gamma_{\max}$. For the various values of γ defined above, we thus have the ordering

$$\gamma_m \leq \gamma_{\min} < \gamma_z < \gamma_* < \gamma_0 < \gamma_1 < \gamma_2 = \gamma_{\max} \,. \tag{3.140}$$

An analytical expression for γ_0 can be found by using the definitions (3.116)–(3.117), and solving $\Psi^2(\gamma) = 1$ for γ. Again, since we know that $\gamma_0 > 0$, no information is lost by squaring. Let us define the auxiliary expression

$$\alpha \equiv \sqrt{8\,\beta_1\,H_2\,H_3 + \left({\beta_1}^2 - 6\,\beta_1\,\beta_2 + {\beta_2}^2\right)\,{H_2}^2} \,, \tag{3.141}$$

where the β_j are the coefficients that appear in the boundary conditions (3.89)–(3.90). For their expressions in terms of the material parameters, see (3.19).

For the root γ_0 that interests us, the following expression holds:

$$\gamma_0^2 = \frac{1}{2}\left((\beta_2 - \beta_1)\,\alpha + 2\,H_1 - \left({\beta_1}^2 - 4\,\beta_1\,\beta_2 + {\beta_2}^2\right)\,H_2 - 4\,\beta_1\,H_3\right) \,. \tag{3.142}$$

Next we will look into some detailed properties of the functions Φ and Ψ, which appear in the minimal symmetric eigenvalue equation for the orthotropic

case, (3.115). Then, to finish the orthotropic problem, we will show some numerical examples.

3.5.5 Analysis of Solution Properties

Let us show that the transcendental part Φ is monotonically decreasing in the open interval $(\lambda_m, \lambda_{max})$. First, we define

$$g(\lambda) \equiv \sqrt{1 - \frac{H_2(H_1 - \lambda)}{H_3^2}} , \tag{3.143}$$

i.e. the square root expression in $\kappa_\pm^2$ in (3.102). We see that $g(\lambda_m) = 0$ and $g(\lambda_{max}) = 1$. Between these extreme values, $g(\lambda)$ increases monotonously as λ increases.

We write (3.102) in the form

$$\kappa_\pm^2 = \frac{1}{dH_3} \left(1 \pm \sqrt{1 - d\,(1 - \lambda)}\right) , \tag{3.144}$$

where we have defined the auxiliary constant

$$d \equiv H_2/H_3^2 .$$

Differentiating (3.144), we have

$$\frac{\partial(\kappa_\pm^2)}{\partial\lambda} = \frac{\pm 1}{2H_3\sqrt{1 - d(1 - \lambda)}} , \tag{3.145}$$

where the upper and lower signs correspond to each other. Note that the square root expression in the denominator is $g(\lambda)$ defined by (3.143), and as discussed above, it takes values in the range (0, 1) as $\lambda \in (\lambda_m, \lambda_{max})$, and especially, is positive in our range of interest. Thus, (3.145) is always positive for κ_+^2 and always negative for κ_-^2.

On the other hand, by the rules of differentiation,

$$\frac{\partial(\kappa_\pm^2)}{\partial\lambda} = 2\kappa_\pm \frac{\partial\kappa_\pm}{\partial\lambda} , \tag{3.146}$$

and thus

$$\frac{\partial\kappa_\pm}{\partial\lambda} = \frac{\partial(\kappa_\pm^2)}{\partial\lambda} / 2\kappa_\pm . \tag{3.147}$$

Noting that $\kappa_\pm > 0$, we can conclude that the signs match:

$$\operatorname{sign}\frac{\partial\kappa_{\pm}}{\partial\lambda}=\operatorname{sign}\frac{\partial(\kappa_{\pm}^{2})}{\partial\lambda}\ . \tag{3.148}$$

In the special case of $\lambda=\lambda_{\max}$, we have $\kappa_{-}=0$, rendering the right-hand side of (3.147) singular, but this point is not in our open interval. Now we turn our attention to the transcendental function Φ. Differentiating (3.116) with respect to λ, we have

$$\begin{aligned}\frac{\partial\Phi}{\partial\lambda}&=\frac{\partial}{\partial\lambda}\left(\tanh\frac{\kappa_{-}}{\mu}\right)\coth\frac{\kappa_{+}}{\mu}\ +\ \left(\tanh\frac{\kappa_{-}}{\mu}\right)\frac{\partial}{\partial\lambda}\left(\coth\frac{\kappa_{+}}{\mu}\right)=\\ &\frac{1}{\cosh^{2}\frac{\kappa_{-}}{\mu}}\cdot\frac{1}{\mu}\cdot\frac{\partial\kappa_{-}}{\partial\lambda}\coth\frac{\kappa_{+}}{\mu}\ +\ \tanh\frac{\kappa_{-}}{\mu}\left(-\frac{1}{\sinh^{2}\frac{\kappa_{+}}{\mu}}\right)\cdot\frac{1}{\mu}\cdot\frac{\partial\kappa_{+}}{\partial\lambda}\ .\end{aligned} \tag{3.149}$$

In the first term on the right-hand side,

$$\frac{\partial\kappa_{-}}{\partial\lambda}<0\ , \tag{3.150}$$

by (3.145) and (3.148), while the other factors are all positive, and in the second term,

$$-\frac{1}{\sinh^{2}\frac{\kappa_{+}}{\mu}}<0\ , \tag{3.151}$$

while all other factors are positive. Thus, both terms on the right side are negative and we conclude that

$$\frac{\partial\Phi}{\partial\lambda}<0\quad\text{for all}\quad\lambda\in(\lambda_{\mathrm{m}},\lambda_{\max})\ . \tag{3.152}$$

Consider now the algebraic function Ψ. We will show the following properties:

1. The function Ψ has exactly one zero at λ_{z}.
2. The function Ψ has exactly one singularity, which is located at $\lambda=\lambda_{\max}$, and its sign is positive:
$$\lim_{\lambda\to\lambda_{\max}}\Psi(\lambda)=+\infty\ .$$
3. If the root $\lambda_{\mathrm{z}}\in(\lambda_{\mathrm{m}},\lambda_{\max})$, then the function Ψ is monotonically decreasing in the interval $\lambda\in(\lambda_{\mathrm{m}},\lambda_{\mathrm{z}})$, and monotonically increasing in the interval $\lambda\in(\lambda_{\mathrm{z}},\lambda_{\max})$.

Again, we begin with (3.102). The coefficient in front of the expression can be written as

$$\frac{H_3}{H_2}=\frac{D_3}{D_2}=\nu_{12}+2\frac{G_{12}}{E_2}\left(1-\nu_{12}\nu_{21}\right)\ . \tag{3.153}$$

By defining the constants

$$A \equiv \frac{H_3}{H_2} = \nu_{12} + 2\frac{G_{12}}{E_2}(1 - \nu_{12}\nu_{21}) \ , \quad B \equiv 2\frac{G_{12}}{E_2}(1 - \nu_{12}\nu_{21}) \ , \tag{3.154}$$

we see that

$$\beta_1 = A - B \ , \qquad \beta_2 = A + B \ . \tag{3.155}$$

Using (3.154) and (3.143), the definition (3.102) reduces to a more convenient form,

$$\kappa_\pm^2 = A(1 \pm g(\lambda)) \ . \tag{3.156}$$

Inserting (3.155) and (3.156) into the definition (3.117), we have

$$\Psi = \frac{\sqrt{A(1 + g(\lambda))}(A\, g(\lambda) - B)^2}{\sqrt{A(1 - g(\lambda))}(A\, g(\lambda) + B)^2} \ . \tag{3.157}$$

All factors in the representation (3.157) are always positive, except the second one in the numerator. Thus, the function can only have one zero, which is located at such λ_z that

$$A\, g(\lambda_z) - B = 0 \ . \tag{3.158}$$

The first result is therefore established.

To show the second result, we note that there is exactly one singularity, caused by the first term in the denominator as $g(\lambda) \to 1$, i.e. as $\lambda \to \lambda_{\max}$. The function Ψ is continuous outside its singularities. Furthermore, from (3.157), we have that $\Psi \geq 0$ for all λ for which the function is nonsingular. Because Ψ is continuous, the singularity must have a positive sign.

To prove the last result we consider the derivative of the function Ψ with regard to λ. Consider the case where

$$\lambda_z \in (\lambda_m, \lambda_{\max}) \ . \tag{3.159}$$

Before we proceed, a motivation of (3.159) may be in order. If $\nu_{12} = 0$, by (3.154) we then have $A = B$. Using (3.158), this leads to $g(\lambda_z) = 1$, and further by (3.143), to $\lambda_z = 1 = \lambda_{\max}$. To see this, observe that $\Psi(\lambda_{\max})$ becomes nonsingular if $A = B$, by considering the limit of (3.157) as $g(\lambda) \to 1^-$. When $A = B$, the second term in the numerator can be rewritten as $(Ag(\lambda) - B)^2 = (B - Ag(\lambda))^2 = A^2(1 - g(\lambda))^2$ and hence, by cancelling the common factor $\sqrt{A(1 - g(\lambda))}$, we are left with $[A(1 - g(\lambda))]^{3/2}$ in the numerator. Thus, for the special case $A = B$, we have $\Psi(\lambda_{\max}) = 0$.

If the case $\lambda_z = \lambda_{\max}$ is allowed to occur, then by the below argument (which works also for this case almost as-is), we will find that Ψ monotonically decreases in the whole open interval $\lambda \in (\lambda_m, \lambda_{\max})$. In such a case, we can no longer be sure that there will exist a point $\lambda = \lambda_*$ in $(\lambda_m, \lambda_{\max})$ satisfying $\Phi(\lambda_*) = \Psi(\lambda_*)$, since both functions then are monotonically decreasing in the whole open interval. Hence, if $\lambda_z = \lambda_{\max}$ is allowed, we cannot say anything about whether a solution of (3.115)

will exist in our interval. Thus, we will limit our consideration to the case $\nu_{12} > 0$ (ensuring $A > B$), which holds for nearly all naturally occurring materials.

We obtain from (3.157), by direct calculation, that

$$\frac{\partial \Psi}{\partial \lambda} = \frac{\partial g}{\partial \lambda} \frac{(B - A\, g(\lambda))}{(B + A\, g(\lambda))^3} \frac{\sqrt{A(1 - g(\lambda))}}{\sqrt{A(1 + g(\lambda))}} \frac{\left(B^2 - A^2 g(\lambda)^2 + 4\, A\, B(g(\lambda)^2 - 1)\right)}{(1 - g(\lambda)^2)}. \tag{3.160}$$

Because all other terms are positive, we have for the sign of the derivative the expression

$$\text{sign} \frac{\partial \Psi}{\partial \lambda} = \text{sign} \left[(B - A\, g(\lambda)) \left(B^2 - A^2 g(\lambda)^2 + 4\, A\, B(g(\lambda)^2 - 1) \right) \right] . \tag{3.161}$$

Because $g(\lambda)$ is monotonically increasing and therefore $\partial g / \partial \lambda > 0$, and the zero of the function Ψ is located at $A\, g(\lambda_z) = B$, we see that

$$\text{sign } [A\, g(\lambda) - B] = \text{sign } [\lambda - \lambda_z] , \tag{3.162}$$

i.e. the sign of the expression $A\, g(\lambda) - B$ corresponds to whether λ is smaller or larger than λ_z.

We can write the expression on the right-hand side of (3.161) as

$$(B - A\, g(\lambda)) \left[(B - A\, g(\lambda))\, (B + A\, g(\lambda)) + 4\, A\, B \left(g(\lambda)^2 - 1 \right) \right] . \tag{3.163}$$

If

$$B - A\, g(\lambda) < 0 \qquad \text{i.e.} \qquad \lambda > \lambda_z , \tag{3.164}$$

the expression in the parentheses at right is negative. The last term is always negative because $g(\lambda) < 1$. In this case we have

$$\frac{\partial \Psi}{\partial \lambda} |_{\lambda > \lambda_z} > 0 . \tag{3.165}$$

The other case

$$B - A\, g(\lambda) > 0 \qquad \text{i.e.} \qquad \lambda < \lambda_z , \tag{3.166}$$

is trickier because then the expression in the parentheses at right in (3.163) will have one positive and one negative term. However, we see that the expression represents a parabola with the variable $g(\lambda)$, having zeroes at

$$g_0^{\pm} \equiv \pm \sqrt{\frac{4AB - B^2}{4AB - A^2}} . \tag{3.167}$$

Because $g(\lambda) > 0$, we may discard the negative solution g_0^- in (3.167). The expression is negative until $g(\lambda)$ becomes larger than the positive solution g_0^+.

The last question remaining is whether this solution lies within our range. Consider the square root expression on the right-hand side of (3.167). We subtract the denominator from the numerator, looking again at the definitions (3.154), and recall that we required $\nu_{12} > 0$:

$$(4AB - B^2) - (4AB - A^2) = A^2 - B^2 > 0 \,,$$

i.e. we find that the numerator is always larger than the denominator. Thus $g_0^+ > 1$ and the parabola remains negative in our entire range. The total sign is negative and thus

$$\frac{\partial \Psi}{\partial \lambda}|_{\lambda<\lambda_z} < 0 \,,$$

which was to be shown.

We will illustrate the critical divergence velocities and the corresponding buckling modes (divergence modes) of axially moving orthotropic plates by giving some

Table 3.3 Physical parameters used in the numerical examples

T_0	m	h
500 N/m	0.08 kg/m^2	10^{-4} m

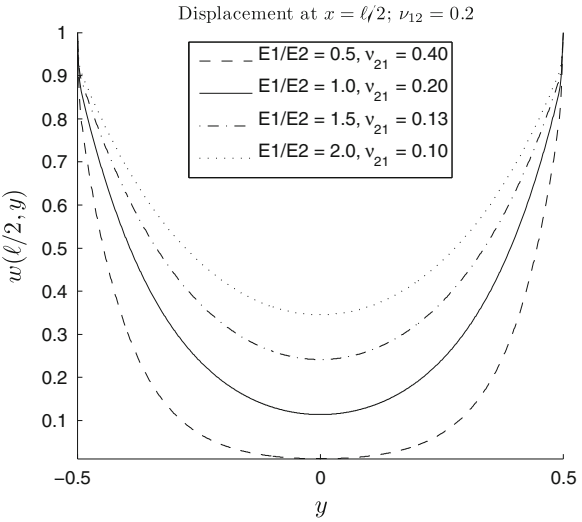

Fig. 3.8 Slices of buckling modes for different Young modulus ratios. Slices of the buckling modes at $x = \ell/2$ are shown. The ratio between the plate length and the plate width is $\ell/(2b) = 0.01$. The Young modulus in the x direction is $E_1 = 5$ GPa and the Poisson ratio ν_{12} is 0.2. The Poisson ratio ν_{21} is calculated from relation (2.36). For the shear modulus, the geometric average G_{H} from (2.25) is used. (Reproduced from Banichuk et al. 2011a)

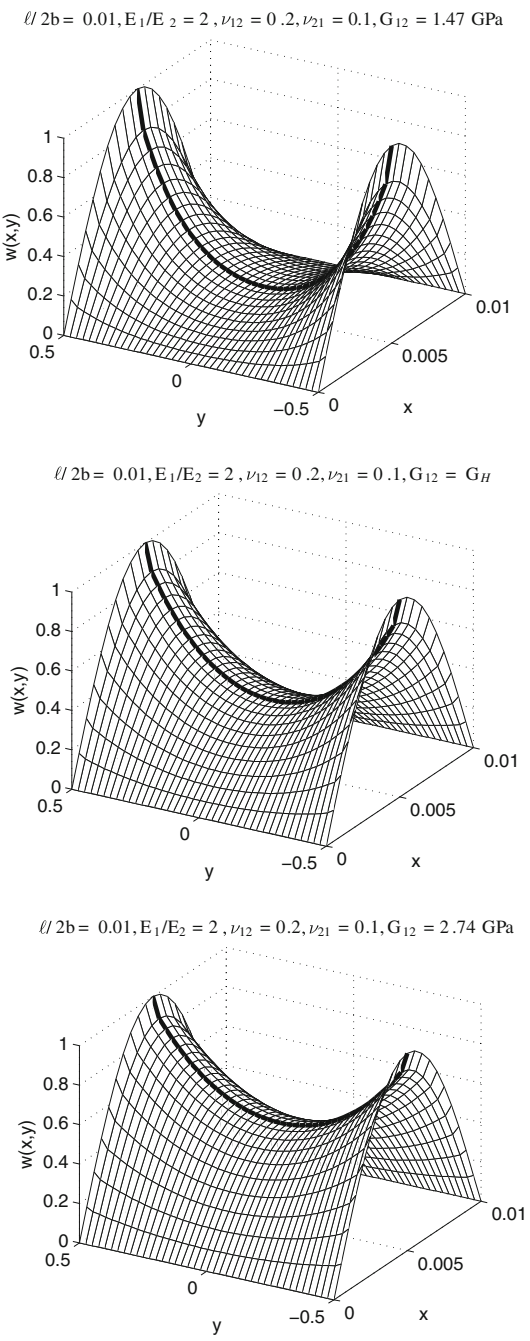

Fig. 3.9 Buckling modes for three different in-plane shear moduli. The ratio between the plate length and the plate width is $\ell/(2b) = 0.01$. *Top* $G_{12} = 0.7G_{\mathrm{H}}$; *Middle* $G_{12} = G_{\mathrm{H}}$; *Bottom* $G_{12} = 1.3G_{\mathrm{H}}$, where G_{12} is the in-plane shear modulus and G_{H} is the geometric average shear modulus, (3.107). The Young moduli are $E_1 = 6.8\,\mathrm{GPa}$ and $E_2 = 3.4\,\mathrm{GPa}$, and the Poisson ratio ν_{12} is 0.2. The Poisson ratio ν_{21} is calculated from relation (2.36), leading to $\nu_{21} = 0.1$. (Reproduced from Banichuk et al. 2011a)

Table 3.4 Critical velocities V_0^{div} (m/s) of an axially moving orthotropic plate for different values of in-plane shear modulus G_{12} and the ratio between the plate length and the plate width $\ell/(2b)$

$\ell/(2b)$	G_{12}		
	$0.7G_{\text{H}} \approx 1.47$ GPa	$G_{\text{H}} \approx 2.11$ GPa	$1.3G_{\text{H}} \approx 2.74$ GPa
0.01	83.4456 m/s	83.4461 m/s	83.4463 m/s
0.1	79.1020 m/s	79.1020 m/s	79.1020 m/s
1	79.0574 m/s	79.0574 m/s	79.0574 m/s

G_{H} is the geometric average shear modulus, (3.107). The Young moduli are $E_1 = 6.8$ GPa and $E_2 = 3.4$ GPa, and the Poisson ratios ν_{12} is 0.2 and $\nu_{21} = 0.1$

numerical examples. The physical parameters used are varied with the examples. The mass per unit area m, the value of homogeneous tension T_0 and the plate thickness h are kept constant, and the used values for them are given in Table 3.3.

In Fig. 3.8, slices of buckling modes at $x = \ell/2$ are presented for four different Young modulus ratios E_1/E_2. We observe that the Young modulus ratio affects the localisation of the buckling mode: the smaller the ratio is, the more the shape is localised near the edges.

The degree of localisation represents the variation of the displacement in the width (y) direction. Relative localisation is high, when most of the displacement occurs near the free edges. The problem parameters affecting the degree of localisation are the aspect ratio $\ell/(2b)$ (as was seen in Sect. 3.4.3), the Young modulus ratio E_1/E_2, the Poisson ratio ν_{12}, and the in-plane shear modulus G_{12}.

In Fig. 3.9, we see three examples of complete buckling shapes for different values of the shear modulus G_{12}. The buckling shapes depend significantly on the in-plane shear modulus G_{12}. The figure also shows that if the ratio G_{12}/G_{H} is increased, then the degree of localisation decreases.

In Table 3.4, the values of critical velocities, defined in (3.123), are given for some selected values of the in-plane shear modulus G_{12} and the aspect ratio $\ell/(2b)$. The row $\ell/(2b) = 0.01$ corresponds to the buckling modes in Fig. 3.9. The effect of the increased in-plane shear modulus is that the value of the critical velocity slightly increases.

References

Alava M, Niskanen K (2006) The physics of paper. Rep Prog Phys 69(3):669–723

Archibald FR, Emslie AG (1958) The vibration of a string having a uniform motion along its length. ASME J Appl Mech 25:347–348

Banichuk N, Jeronen J, Neittaanmäki P, Tuovinen T (2010a) On the instability of an axially moving elastic plate. Int J Solids Struct 47(1):91–99. http://dx.doi.org/10.1016/j.ijsolstr.2009.09.020

Banichuk N, Jeronen J, Neittaanmäki P, Tuovinen T (2010b) Static instability analysis for travelling membranes and plates interacting with axially moving ideal fluid. J Fluids Struct 26(2):274–291. http://dx.doi.org/10.1016/j.jfluidstructs.2009.09.006

Banichuk N, Jeronen J, Kurki M, Neittaanmäki P, Saksa T, Tuovinen T (2011a) On the limit velocity and buckling phenomena of axially moving orthotropic membranes and plates. Int J Solids Struct 48(13):2015–2025. http://dx.doi.org/10.1016/j.ijsolstr.2011.03.010

Banichuk N, Jeronen J, Neittaanmäki P, Tuovinen T (2011b) Dynamic behaviour of an axially moving plate undergoing small cylindrical deformation submerged in axially flowing ideal fluid. J Fluids Struct 27(7):986–1005. http://dx.doi.org/10.1016/j.jfluidstructs.2011.07.004

Banichuk N, Jeronen J, Neittaanmäki P, Saksa T, Tuovinen T (2013) Theoretical study on travelling web dynamics and instability under non-homogeneous tension. Int J Mech Sci 66C:132–140. http://dx.doi.org/10.1016/j.ijmecsci.2012.10.014

Biancolini ME, Brutti C, Reccia L (2005) Approximate solution for free vibrations of thin orthotropic rectangular plates. J Sound Vibr 288(1–2):321–344. doi:10.1016/j.jsv.2005.01.005

Bolotin VV (1963) Nonconservative problems of the theory of elastic stability. Pergamon Press, New York

Bonnin A, Huchon R, Deschamps M (2000) Ultrasonic waves propagation in absorbing thin plates: application to paper characterization. Ultrasonics 37(8):555–563. http://dx.doi.org/10.1016/S0041-624X(99), 00106–7

Chang YB, Moretti PM (1991) Interaction of fluttering webs with surrounding air. TAPPI J 74(3):231–236

Chen G, Coleman MP, Ding Z (1998) Some corner effects on the loss of selfadjointness and the non-excitation of vibration for thin plates and shells. Q J Mech Appl Math 51(2):213–240. doi:10.1093/qjmam/51.2.213

Chen LQ, Ding H (2010) Steady-state transverse response in coupled planar vibration of axially moving viscoelastic beams. ASME J Vibr Acoust 132:011,009–1-9. http://dx.doi.org/10.1115/1.4000468

Chen LQ, Wang B (2009) Stability of axially accelerating viscoelastic beams: asymptotic perturbation analysis and differential quadrature validation. Eur J Mech Solids 28(4):786–791. doi:10.1016/j.euromechsol.2008.12.002

Chen LQ, Zhao WJ (2005) A numerical method for simulating transverse vibrations of an axially moving string. Appl Math Comput 160(2):411–422. doi:10.1016/j.amc.2003.11.012

Chen LQ, Chen H, Lim C (2008) Asymptotic analysis of axially accelerating viscoelastic strings. Int J Eng Sci 46(10):976–985. doi:10.1016/j.ijengsci.2008.03.009

Chonan S (1986) Steady state response of an axially moving strip subjected to a stationary lateral load. J Sound Vibr 107:155–165

Ding H, Chen LQ (2008) Stability of axially accelerating viscoelastic beams: multi-scale analysis with numerical confirmations. Eur J Mech Solids 27(6):1108–1120. doi:10.1016/j.euromechsol.2007.11.014

Erkkilä AL, Leppänen T, Hämäläinen J (2013) Empirical plasticity models applied for paper sheets having different anisotropy and dry solids content levels. Int J Solids Struct in press. http://dx.doi.org/10.1016/j.ijsolstr.2013.03.004

Euler L (1766) De motu vibratorio tympanorum. Novi Commentarii academiae scientiarum imperialis Petropolitanae 10:243–260. http://eulerarchive.maa.org/pages/E302.html

Frondelius T, Koivurova H, Pramila A (2006) Interaction of an axially moving band and surrounding fluid by boundary layer theory. J Fluids Struct 22(8):1047–1056

Fung RF, Huang JS, Chen YC (1997) The transient amplitude of the viscoelastic travelling string: an integral constitutive law. J Sound Vibr 201(2):153–167. doi:10.1006/jsvi.1996.0776

Fung RF, Huang JS, Chen YC, Yao CM (1998) Nonlinear dynamic analysis of the viscoelastic string with a harmonically varying transport speed. Comput Struct 66(6):777–784. doi:10.1016/S0045-7949(98)00001-7

Gorman DJ (1982) Free vibration analysis of rectangular plates. Elsevier North Holland, Inc. ISBN 0-444-00601-X.

Göttsching L, Baumgarten HL (1976) Triaxial deformation of paper under tensile load. In: The fundamental properties of paper related to its uses, vol 1. Technical Division of the British Paper and Board Industry Federation, pp 227–252

Hatami S, Azhari M, Saadatpour MM, Memarzadeh P (2009) Exact free vibration of webs moving axially at high speed. In: AMATH'09: proceedings of the 15th American conference on applied mathematics. World Scientific and Engineering Academy and Society (WSEAS), Stevens Point, Wisconsin, USA, pp 134–139, houston, USA

Hosaka H, Crandall SH (1992) Self-excited vibrations of a flexible disk rotating on an air film above a flat surface. Acta Mech 3:115–127 (supplement)

Jeronen J (2011) On the mechanical stability and out-of-plane dynamics of a travelling panel submerged in axially flowing ideal fluid: a study into paper production in mathematical terms. PhD thesis, Department of Mathematical Information Technology, University of Jyväskylä. http://julkaisut.jyu.fi/?id=978-951-39-4596-1, Jyväskylä studies in computing 148. ISBN 978-951-39-4595-4 (book), ISBN 978-951-39-4596-1 (PDF)

Kong L, Parker RG (2004) Approximate eigensolutions of axially moving beams with small flexural stiffness. J Sound Vibr 276:459–469

Kshirsagar S, Bhaskar K (2008) Accurate and elegant free vibration and buckling studies of orthotropic rectangular plates using untruncated infinite series. J Sound Vibr 314(3–5):837–850. doi:10.1016/j.jsv.2008.01.013

Kulachenko A, Gradin P, Koivurova H (2007a) Modelling the dynamical behaviour of a paper web. Part I Comput Struct 85:131–147

Kulachenko A, Gradin P, Koivurova H (2007b) Modelling the dynamical behaviour of a paper web. Part II. Comput Struct 85:148–157

Kurki M, Lehtinen A (2009) In-plane strain field theory for 2-d moving viscoelastic webs. In: Papermaking research symposium 2009 (Kuopio, Finland), PRS

Lee U, Oh H (2005) Dynamics of an axially moving viscoelastic beam subject to axial tension. Int J Solids Struct 42(8):2381–2398. http://dx.doi.org/10.1016/j.ijsolstr.2004.09.026

Lin CC (1997) Stability and vibration characteristics of axially moving plates. Int J Solids Struct 34(24):3179–3190

Lin CC, Mote CD (1995) Equilibrium displacement and stress distribution in a two-dimensional, axially moving web under transverse loading. ASME J Appl Mech 62:772–779

Lin CC, Mote CD (1996) Eigenvalue solutions predicting the wrinkling of rectangular webs under non-linearly distributed edge loading. J Sound Vibr 197(2):179–189

Mann RW, Baum GA, Habeger CC (1980) Determination of all nine orthotropic elastic constants for machine-made paper. TAPPI J 63(2):163–166

Marynowski K (2008) Dynamics of the axially moving orthotropic web, vol 38. Lecture notes in applied and computational mechanics. Springer, Germany

Marynowski K, Kapitaniak T (2002) Kelvin-Voigt versus Bürgers internal damping in modeling of axially moving viscoelastic web. Int J Non-Linear Mech 37(7):1147–1161. doi:10.1016/S0020-7462(01)00142-1

Miranker WL (1960) The wave equation in a medium in motion. IBM J Res Dev 4:36–42

Mockensturm EM, Guo J (2005) Nonlinear vibration of parametrically excited, viscoelastic, axially moving strings. ASME J Appl Mech 72(3):374–380. doi:10.1115/1.1827248

Mote CD (1972) Dynamic stability of axially moving materials. Shock Vibr Digest 4(4):2–11

Mote CD Jr, Wickert JA (1991) Response and discretization methods for axially moving materials. Appl Mech Rev 44(11):S279–S284

Mujumdar AS, Douglas WJM (1976) Analytical modelling of sheet flutter. Svensk Papperstidning 79:187–192

Niemi J, Pramila A (1986) Vibration analysis of an axially moving membrane immersed into ideal fluid by FEM. Tampereen teknillinen korkeakoulu (Tampere University of Technology), Tampere, Technical report

Oh H, Cho J, Lee U (2004) Spectral element analysis for an axially moving viscoelastic beam. J Mech Sci Technol 18(7):1159–1168. http://dx.doi.org/10.1007/BF02983290, DOI: 10.1007/BF02983290

Païdoussis MP (1998) Fluid-structure interactions: slender structures and axial flow, vol 1. Academic Press. ISBN 0-12-544360-9

Païdoussis MP (2004) Fluid-structure interactions: slender structures and axial flow, vol 2. Elsevier Academic Press. ISBN 0-12-544361-7
Païdoussis MP (2005) Some unresolved issues in fluid-structure interactions. J Fluids Struct 20(6):871–890
Païdoussis MP (2008) The canonical problem of the fluid-conveying pipe and radiation of the knowledge gained to other dynamics problems across applied mechanics. J Sound Vibr 310:462–492
Parker RG (1998) On the eigenvalues and critical speed stability of gyroscopic continua. ASME J Appl Mech 65:134–140
Pramila A (1986) Sheet flutter and the interaction between sheet and air. TAPPI J 69(7):70–74
Russo L (2004) The forgotten revolution: how science was born in 300 BC and why it had to be reborn. Springer. ISBN 978-3540203964
Sack RA (1954) Transverse oscillations in traveling strings. Br J Appl Phys 5:224–226
Seo YB (1999) Determination of in-plane shear properties by an off-axis tension method and laser speckle photography. J Pulp Pap Sci 25(9):321–325
Shen JY, Sharpe L, McGinley WM (1995) Identification of dynamic properties of plate-like structures by using a continuum model. Mech Res Commun 22(1):67–78
Shin C, Chung J, Kim W (2005) Dynamic characteristics of the out-of-plane vibration for an axially moving membrane. J Sound Vibr 286(4–5):1019–1031
Simpson A (1973) Transverse modes and frequencies of beams translating between fixed end supports. J Mech Eng Sci 15:159–164
Skowronski J, Robertson AA (1985) A phenomenological study of the tensile deformation properties of paper. J Pulp Pap Sci 11(1):J21–J28
Skutch R (1897) Uber die Bewegung eines gespannten Fadens, weicher gezwungen ist durch zwei feste Punkte, mit einer constanten Geschwindigkeit zu gehen, und zwischen denselben in Transversal-schwingungen von gerlinger Amplitude versetzt wird. Annalen der Physik und Chemie 61:190–195
Swope RD, Ames WF (1963) Vibrations of a moving threadline. J Franklin Inst 275:36–55
Sygulski R (2007) Stability of membrane in low subsonic flow. Int J Non-Linear Mech 42(1):196–202
Thorpe JL (1981) Paper as an orthotropic thin plate. TAPPI J 64(3):119–121
Timoshenko SP, Woinowsky-Krieger S (1959) Theory of plates and shells, 2nd edn. McGraw-Hill, New York . ISBN 0-07-085820-9
Tuovinen T (2011) Analysis of stability of axially moving orthotropic membranes and plates with linear non-homogeneous tension profile. PhD thesis, Department of Mathematical Information Technology, University of Jyväskylä, http://julkaisut.jyu.fi/?id=978-951-39-4578-7, Jyväskylä studies in computing 147. ISBN 978-951-39-4577-0 (book). ISBN 978-951-39-4578-7 (PDF)
Wang X (2003) Instability analysis of some fluid-structure interaction problems. Comput Fluids 32(1):121–138
Wang Y, Huang L, Liu X (2005) Eigenvalue and stability analysis for transverse vibrations of axially moving strings based on Hamiltonian dynamics. Acta Mech Sinica 21:485–494
Wickert JA (1992) Non-linear vibration of a traveling tensioned beam. Int J Non-Linear Mech 27(3):503–517
Wickert JA, Mote CD (1990) Classical vibration analysis of axially moving continua. ASME J Appl Mech 57:738–744
Xing Y, Liu B (2009) New exact solutions for free vibrations of rectangular thin plates by symplectic dual method. Acta Mech Sinica 25:265–270
Yang XD, Zhang W, Chen LQ, Yao MH (2012) Dynamical analysis of axially moving plate by finite difference method. Nonlinear Dyn 67(2):997–1006. http://dx.doi.org/10.1007/s11071-011-0042-2
Yokoyama T, Nakai K (2007) Evaluation of in-plane orthotropic elastic constants of paper and paperboard. In: 2007 SEM annual conference & exposition on experimental and applied mechanics